The Journal of Supercritical Fluids 237 (2026) 107061

Contents lists available at ScienceDirect

The Journal of Supercritical Fluids

journal homepage: www.elsevier.com/locate/supflu

Supercritical CO_2-assisted impregnation of triamcinolone acetonide into silicone-based soft contact lenses for enhanced ocular drug delivery

Diana C. Silva [a,b,*,1], Margarida Gonçalves [a,1], Elisabeth Ekoh [a], Madalena Salema-Oom [b], Ana Paula Serro [a,b], Beatriz P. Nobre [a,c,*]

[a] Centro de Química Estrutural (CQE), Institute of Molecular Sciences, Departamento de Engenharia Química, Instituto Superior Técnico, Universidade de Lisboa, Av. Rovisco Pais, Lisboa 1049-001, Portugal
[b] Egas Moniz Center for Interdisciplinary Research, Egas Moniz School of Health & Science, Quinta da Granja, Monte de Caparica, Caparica 2829-511, Portugal
[c] Departamento de Engenharia Química, Instituto Superior de Engenharia de Lisboa, Instituto Politécnico de Lisboa, Rua Conselheiro Emídio Navarro, 1, Lisboa 1959-007, Portugal

HIGHLIGHTS

- Temperature and pressure are key factors in SCI of TA in silicone hydrogel lenses.
- TA-impregnated SCLs showed > 90% transmittance and suitable properties.
- No cytotoxicity or irritability was observed in TA-loaded SCI hydrogels.

GRAPHICAL ABSTRACT

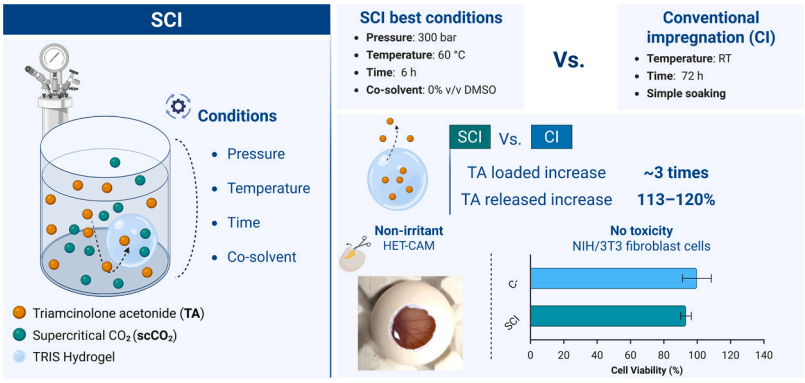

ARTICLE INFO

Keywords:
Supercritical carbon dioxide
Soft contact lenses
Drug delivery
Triamcinolone acetonide

ABSTRACT

Soft contact lenses (SCLs) have attracted increasing attention in the field of ocular drug delivery systems, owing to their potential to improve drug bioavailability *in vivo*. However, the incorporation of lipophilic drugs, constitutes a significant challenge through conventional soaking methods. Supercritical carbon dioxide ($scCO_2$), an environmentally friend solvent, has emerged as an efficient alternative for the development of delivery systems improving the impregnation of such drugs. In this work, $scCO_2$ impregnation (SCI) was employed to load silicone-based hydrogels for SCLs, with triamcinolone acetonide (TA), a lipophilic corticosteroid. Design of experiments was conducted using a full factorial design to identify the most significant experimental parameters affecting TA SCI, as well as to predict the experimental conditions that maximise SCI. In vitro release assays were carried out with materials loaded by SCI and by conventional soaking. The best performing materials were subjected to an extensive characterisation (thermal behaviour, and optical, physical, chemical and mechanical properties). The

* Corresponding authors at: Centro de Química Estrutural (CQE), Institute of Molecular Sciences, Departamento de Engenharia Química, Instituto Superior Técnico, Universidade de Lisboa, Av. Rovisco Pais, Lisboa 1049-001, Portugal.
E-mail addresses: dianacristinasilva@tecnico.ulisboa.pt (D.C. Silva), maria.nobre@isel.pt (B.P. Nobre).
[1] Equal Authorship

https://doi.org/10.1016/j.supflu.2026.107061
Received 16 January 2026; Received in revised form 2 June 2026; Accepted 8 June 2026
Available online 13 June 2026

results confirmed that TA-loaded SCLs can be effectively prepared using the SCI process. The highest SCI yields were obtained with materials processed at 300 bar and 60 °C, reaching a TA amount released of 10.12 ± 0.44 μg. mg^{-1} dry gel, which represents a 162.2% increase compared to the conventional soaking. SCI hydrogels showed suitable properties for the intended application. Overall, the SCI process proved to be both effective, with potential for further optimisation through condition refinement.

1. Introduction

The development of advanced ocular drug delivery systems has become a critical area of research, aiming to address limitations such as low bioavailability and risks commonly associated with current methods [1]. Traditional ocular drug delivery approaches, like eye drops typically deliver less than 5% of the administered drug to the target tissue, with the majority lost through tear turnover or nasolacrimal drainage. To achieve therapeutic concentrations, frequent application or high dosages are often required, which may lead to loss of patients compliance and undesirable side effects, especially in the context of long-term treatment [2,3]. In turn, intraocular injections, frequently used in the treatment of posterior eye diseases are quite effective, but are invasive procedures that carry significant risks, including retinal detachment, intravitreal haemorrhage, and cataract formation [4].

Therapeutic contact lenses have emerged as a promising alternative for ocular drug delivery [5], offering enhanced bioavailability (up to 50%) and improved patient compliance while reducing the side effects associated with eye drops and injections [6]. This strategy is particularly appealing for drugs typically administered via intravitreal injections, as it is safer. The treatment of retinal disorders such as diabetic retinopathy, diabetic macular edema, and age-related macular edema often involves the administration of corticosteroids like triamcinolone acetonide (TA) via intravitreal injections [7]. Soft contact lenses (SCLs) are particularly suitable platforms for drug incorporation, often using simple methods like soaking in concentrated drug solutions. However, the poor water solubility of TA poses a significant limitation for drug loading through conventional soaking [8]. Manufacturing methods have been extensively applied to improve drug loading and release kinetics: molecular imprinting [9], surface modification [10], coatings [11,12], nanoparticle incorporation [13], cyclodextrins complex formation [14], or the use of organic solvents [15]. However, many of these methods do not offer scalability and involve multiple and complex technical, regulatory and economic challenges [5,16,17].

Supercritical carbon dioxide ($scCO_2$) impregnation (SCI) emerges as a compelling alternative for enhancing drug loading in SCLs, namely of hydrophobic drugs. This method leverages the unique properties of $scCO_2$, such as low viscosity, high diffusivity, and tuneable solvent power, to impregnate drugs into polymeric materials without the use of harmful organic solvents [18]. SCI is regulated by two primary mechanisms: one involves deposition of the drug as solid particles within the polymer matrix (supercritical fluid deposition), and the other involves molecular dispersion of the drug throughout the polymer (true impregnation), generally resulting in higher drug loading compared to soaking [19]. A key advantage of SCI lies in its process tuneability. Operational parameters such as pressure, temperature, impregnation time, and co-solvent composition can be precisely adjusted to optimise drug loading and release characteristics. This makes SCI a versatile and efficient approach, particularly for hydrophobic or poorly water-soluble drugs like TA [20]. Recent studies have validated the feasibility of SCI for drug loading in various commercial SCLs and intraocular lenses (IOLs), demonstrating that drug loading can be effectively controlled by modulating process parameters [21–23]. Many of these studies focused on commercial acrylate or silicone-based SCLs impregnated with anti-glaucoma drugs such as timolol maleate, or anti-bacterial agents like moxifloxacin [24,25]. Notably, a pioneering effort in Portugal led to the development and patenting of the SCI process for ophthalmic devices (EP 1 611877 A1) [26]. Costa *et al.* [22] investigated the SCI of several commercial SCLs (Nelifilcon A, Hilafilcon B, Methafilcon A, Omafilcon A) using both hydrophobic (flurbiprofen) and hydrophilic (timolol maleate) drugs. Impregnation was performed at pressures ranging from 9 MPa to 16 MPa, for periods between 30 min and 180 min, at 40 °C. The results confirmed that therapeutic drug levels were achieved while maintaining lens transparency and eliminating solvent residues. Importantly, drug loading times were significantly reduced from up to a week using soaking methods to just 2 h with SCI. In subsequent work, Costa *et al.* [20] studied the SCI of Balafilcon A SCLs with acetazolamide (hydrophobic) and timolol maleate (hydrophilic), using conditions of 17 MPa, 40 °C, and 90 min. Co-solvents such as ethanol and water at concentrations of (5, 10, 15) mol% were employed to improve drug solubility and control loading efficiency. The process maintained crucial lens properties, including oxygen permeability and glass transition temperature (T_g). Building on these findings, Braga *et al.* [21] investigated acetazolamide impregnation into Balafilcon A lenses using ethanol (5 mol%) as a co-solvent. By adjusting parameters such as pressure (15–20 MPa), temperature (40–50 °C), duration (1–3 h), and depressurisation rate (0.06–0.15 MPa·min^{-1}), they achieved therapeutic drug levels without compromising the thermomechanical or optical properties of the lenses. González-Chomón *et al.* [27] evaluated the use of norfloxacin-eluting IOLs to tackle post-surgery infections. $scCO_2$-based impregnation method was implemented to improve the uptake of norfloxacin, reaching highest loading yield (~1.65 mg norfloxacin/g dry lens) under optimised conditions of 300 bar of pressure, 40 °C, and a 14 h process time. Ongkasin *et al.* [28] used $scCO_2$ to impregnate hydrophobic acrylic IOLs with a fluoroquinolone drug (gatifloxacin). Several conditions were evaluated (8–25 MPa, 35 °C to 55 °C and 30 min to 240 min impregnation duration), in which the impregnation yields ranged 0.33 μg·mg^{-1} and 1.07 ± 0.07 μg·mg^{-1}.

In the present study, a silicone-based hydrogel was developed for the incorporation of therapeutic levels of TA. The hydrogel was subjected to SCI in order to enhance TA solubilisation and impregnation into the polymer matrix. Full factorial design was used to screen the most significant operational parameters; pressure (200–300 bar), temperature (40–60 °C), time of impregnation (2–6 h), and co-solvent concentration (DMSO: 0–5% v/v), and determine the optimal drug loading and release performance. Comprehensive characterisation of the hydrogels before (non-treated, NT) and after SCI was conducted to assess their suitability as SCLs. This included analysis of morphology, optical transparency, chemical composition, thermal behaviour, and mechanical integrity. Biocompatibility tests were also carried out. Ultimately, this work contributes with valuable data and process knowledge that support the development of more efficient, scalable, and commercially relevant SCLs for sustained ocular drug delivery.

2. Experimental

2.1. Materials

3-Tris(trimethylsiloxy)silyl propyl 2-methylprop−2-enoate (TRIS, purity ≥ 98%) and 2-hydroxyethylmethacrylate (HEMA, purity ≥ 99%) stabilised with MEHQ (4-methoxyphenol) were supplied by TCI Chemicals (Tokyo Chemical Industry Co., Ltd., Japan). N-Vinyl pyrrolidone (NVP, purity ≥ 98%), Phosphate buffer saline (PBS) tablets, pH 7.4, Ethylene glycol dimethacrylate (EGDMA, purity ≥ 98%) and 2,2'-azobis (2-methylpropionitrile) (AIBN, purity ≥ 98%), Dulbecco's Modified Eagle Medium (DMEM), foetal bovine serum penicillin-streptomycin

solution, Phosphate Buffered Saline (PBS), trypsin-trypsin ethylenediaminetetraacetic acid (EDTA) solution, 0.4% trypan blue, dimethyl sulfoxide (DMSO), 3-(4,5Dimethylthiazol−2-yl)−2,5-diphenyltetrazolium bromide (MTT), isopropanol and hydrochloric acid (HCl) were obtained from Sigma-Aldrich (Massachusetts, USA). Triamcinoloneacetonide (TA) was supplied by Acofarma (Madrid, Spain). Methanol (CH_3OH, purity $\geq$ 99.9%) was purchased from Carlo Erba (Spain). Distilled and deionised water (DD water, 18 MΩ.cm) was obtained from a Millipore Milli-Q® system. The SCF employed in this work was carbon dioxide (CO_2) (purity $>$ 99.998%) from Air Liquide (Portugal). Dimethyl sulfoxide (DMSO) (purity $\geq$ 99.5%) used as a co-solvent was supplied by Honeywell (Japan). Sodium hydroxide (NaOH) and octylphenoxypoly(ethyleneoxy)ethanol (IGEPAL) were from Merck (Darmstadt, Germany). Sodium chloride (NaCl $\geq$ 99% was purchase from Panreac (Castellar del Vallès, Spain). NIH/3T3 (CRL−1658) fibroblasts were purchased from ATCC (Manassas, Virginia, USA).

2.2. Preparation of SCLs materials

TRIS/NVP/HEMA hydrogels were prepared as the base material for SCLs. First, monomer mixtures (0.8 M TRIS, 3.9 M NVP, 1.8 M HEMA, 30 mM EGDMA) containing 15 mM AIBN were homogenised, with the initiator dissolved in the mixture at room temperature under magnetic stirring. The solution was then degassed with a nitrogen flux for 2 min and sonicated for 5 min. Next, the solution was injected into a mould, constituted of two silanised glass plates coupled with a 0.2 mm Teflon frame separator. Thermal polymerisation was achieved in a dry oven at 60 ºC for 24 h. After polymerisation, the hydrogels were washed by soaking in DD water, renewed three times daily, for five days to remove unreacted monomers. The absence of these toxic monomers was confirmed by ultraviolet-visible (UV-Vis) spectrophotometry (Multiskan GO, Thermo Scientific, Waltham, USA) in a wavelength range of 200 – 700 nm. The obtained samples were cut into 12 mm discs (unless otherwise stated) using a biopsy puncher and then dried at 40 ºC for 48 h prior to storage in closed flasks.

2.3. Supercritical impregnation of SCLs materials

2.3.1. Experimental set-up

Supercritical impregnation experiments (SCI) were performed in a high-pressure cylindrical vessel (300 cm^3 internal volume), as schematically represented in Fig. 1. The high pressure equipment in that was used to carry out the SCI experiments was adapted from [29]. In this apparatus CO_2 enters the high pressure vessel from the top, being previously heated in a thermostatized water bath, in which the high pressure vessel is also immersed. CO_2 is pumped inside the vessel by an HPLC pump and the pressure is set by a back-pressure regulator. The high pressure vessel has a tubing at the bottom with a micrometric valve, which allows to control the CO_2 flow-rate from the vessel. During the impregnation experiments the micrometric valve is close, in order guarantee the desired batch impregnation time.

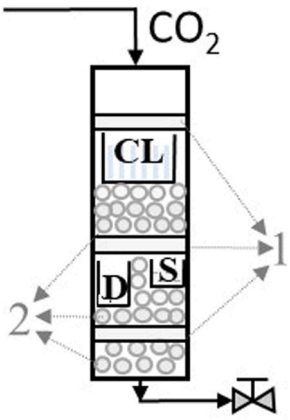

Fig. 1. Schematic representation of the supercritical impregnation pressure vessel layout. CL – cellulose thimble with the soft contact lenses; D - cellulose thimble with the drug (triamcinolone acetonide); S – glass container with co-solvent (DMSO); 1- stainless steel frit; 2- glass beads.

The filling of the high-pressure vessel was prepared, for each run, as follow: before each run, the vessel was filled with two main distinct layers, as shown in Fig. 1. The layer at the top of the vessel has the hydrogel samples to be impregnated and the layer just below has the impregnation drug, as well as the co-solvent for the run that required this condition. The amount of drug (TA) used in each experiment was 20 mg and, for the experiments requiring it, the solvent amount was determined taking into account the concentration required (2.5 or 5.0% v/v) and the CO_2 density for each run (function of pressure and temperature). The layers were separated by stainless steel frit (pore diameter 200 nm). Glass beads (1 cm Ø) were used to create the packing inside the vessel and ensure uniform CO_2 flow and intimate contact between the supercritical fluid and solid phases. The hydrogel samples to be impregnated were placed inside cellulose thimbles (100% cotton linter), in vertical position in order to avoid deposition of the drug over. Eight samples of hydrogel were used in each experiment, and these were placed in 4 different thimbles (2 hydrogels/thimble). The impregnation drug, TA, was placed inside another cellulose thimble. The co-solvent (when necessary) was placed inside a glass cylindrical container (2.5 ×3.5 mm) open at the top. The selected layout (i.e the hydrogels positioned at the top of the vessel, above the position of the drug and of co-solvent) ensured that the drug deposition on the material's surface would be minimised during the depressurisation step.

Moreover, with this layout (Fig. 1), the void fraction inside the vessel was c.a. 0.7, which was determined measuring the total volume of CO_2 required to fill the high-pressure vessel, filled with the hydrogels, the drug and the co-solvent, under the various pressure and temperature conditions studied.

2.3.2. Supercritical Impregnation Experimental Procedure

All experiments carried out in the supercritical CO_2 impregnation equipment followed the experimental this procedure: The high pressure vessel, loaded as described in Section 2.3.1 (Fig. 1), was connected to CO_2 inlet tubing at the top, and both tubing and vessel are placed inside a thermostatically controlled water bath, which was heated to the working temperature. After the operating temperature was reached, CO_2 was pumped into the system using an HPLC pump, being the pressure controlled by a back-pressure regulator. When the CO_2 pressure inside the high-pressure vessel reached the operating value, the required experimental conditions were achieved and the impregnation time count began. The CO_2, at desired temperature and pressure, remained in batch mode inside the high-pressure vessel for the required impregnation time. After completion of impregnation time the system depressurisation was initiated by opening the micrometric valve, located in the tubing at the bottom of the high pressure vessel. Depressurisation was carried out at a controlled rate between 0.1 $bar.min^{-1}$ and 0.2 $bar.min^{-1}$. The supercritical impregnation apparatus has also a rotameter and a wet teste meter, located after the micrometic valve, which allow to measure the CO_2 flow-rate leaving the high pressure vessel and the total amount of CO_2 used in each experiment, respectively. After complete depressurisation of the high-pressure vessel and adjacent tubings, the impregnation vessel was opened and the samples were collected for further analysis.

The SCI experiments using co-solvent, i.e DMSO, followed a slightly different procedure. For these experiments when the impregnation time was completed, it was necessary to submitted the SCI vessel to a drying step, in order to remove the co-solvent that could be inside the hydrogel polymer. The drying step was carried out by passing CO_2, under the pressure and temperature conditions of the previously supercritical

impregnation procedure, and using a very low CO_2 flow rate of 1.4 g/min, in order to avoid drug entrainment. The total drying time was 75 min and was calculated considering that the system behaved as a perfectly stirred reactor under steady-state conditions, taking into account the density the supercritical fluid and of the co-solvent, as well as the solubility of the co-solvent in CO_2. After the drying step was finished the system was then submitted to depressurisation, at a rate kept as described above, 0.1–0.2 bar/min. The total volume of CO_2 used inside the high pressure vessel, varied from 77 L to 97 L (STP), depending on the densitiy of CO_2.

Co-solvent volumes placed inside the vessel were calculated based on the $scCO_2$ density at the selected pressure and temperature conditions and the vessel void fraction (0.7), to achieve final concentrations of 0% v/v to 5%v/v DMSO. Volumes of DMSO placed inside the vessel varied between 6 mL and 16 mL.

The impact of the operating conditions on TA impregnation into the hydrogel was studied by varying the temperature, pressure, time of impregnation and co-solvent concentration in the supercritical fluid phase. DMSO, a GRAS (Generally Recognised as Safe) and Food and Drug Administration class 3 solvent, was selected as a polar modifier to enhance both TA solubility in $scCO_2$ and polymer swelling [30,31], since preliminary experiments previously carried out by the research team showed that other GRAS solvents: ethanol and acetone were ineffective.

2.3.3. Preliminary experiments to Supercritical Impregnation studies

Prior to supercritical impregnation experimental studies, the hydrogel samples underwent a $scCO_2$ treatment (SCT) to assess the effects of temperature (40–60 °C) and pressure (200–300 bar) on their optical transmittance, refractive index, swelling behaviour, and chemical structure. In these experiments only the hydrogels samples were placed inside the high pressure vessel and no drug or co-solvent were used. These preliminary tests defined the safe pressure and temperature operating range for subsequent SCI experiments. Success criteria included preserved lens material's properties and absence of visible damage. Once proved the resistance of material, the drug impregnation studies were performed.

2.3.4. Full factorial design

A four-variable, 2-level full-factorial design (FFD) was employed to identify the primary factors governing drug release and impregnation yield. The design of experiments (DoE) through the 2-level FFD is commonly used in screening experiments and aims to identify the relation between the experimental factors and the response variables and determine the most significant experimental factors influencing the response variables, enabling the prioritising of the experimental factors in further optimisation studies. This design also aids to identify the interactions between experimental factors. In DoE a 2-level FFD indicates that each experimental factor has two levels, which are the specific values the factor can take, typically labelled as "low" and "high", corresponding to the minimum and maximum values of the experimental parameter within the range considered for the study. These 2 levels of the experimental factors can also be assigned with the coded values taking the value of −1 and + 1, for the low and high level, respectively. A centre point (middle point of the considered parameter's range, with code value 0) can also be added to the DoE matrix, enabling some curvature effect [21,22,32].

- The Software Design-Expert® (version 13.0 software by Stat-Ease Inc. located in Minneapolis, MN, USA) was used to generate a randomised matrix of 16 (2^4) experimental runs, which include the centre point for all parameters. This software was also used to evaluate the DoE experimental results, and thus to carry out the data analysis and the model building. All runs were performed in duplicate. The generated matrix included three repetitions of the centre point. An additional run with intermedium parameters values was also carried out to minimise the influence of nuisance variables [32].

The chosen response variables were:

- Y1: Cumulative drug released at 72 h of drug release experiment (μg.$mg^{-1}$of dried gel)
- Y2: Drug amount loaded (μg.$mg^{-1}$of dried gel).

The experimental factors to be studied were: pressure, temperature, time of impregnation and co-solvent amount.

Pressure (200–300 bar) and temperature (40–60 °C) low and high levels were defined based on published SCI studies in silicone-based hydrogels [33] and TA solubility data in $scCO_2$ [30]. Co-solvent concentration was set at 0% v/v (no co-solvent) for the low level and 5% v/v (the minimum fraction that demonstrated to enhance SCI) for the high level. Impregnation time high level was set based in considering less than 8 h shift and the low level was defined based on the average low impregnation time reported in literature for SC impregnation of contact lenses [22–26,28]. The obtained randomised matrix of experimental runs depicting the real (i.e. uncoded) levels of the four independent experimental parameters is presented in Table 1. The nomenclature used for the several prepared samples, which will be useful to follow the results analysis section, can also be consulted in this table.

2.4. Conventional impregnation

Dried hydrogel discs (n = 4) not subjected to SCT were immersed individually in falcon tubes with 1 mL of TA solution (1 mg.mL^{-1} in PBS), at room temperature. The samples were left soaking for 2 h (NT_TA_2h), 4 h (NT_TA_4h), 6 h (NT_TA_6h) and 72 h (NT_TA_72h), for comparison purposes. The impregnation time of 72 h was selected based on its widespread use in the literature as a standard condition for conventional soaking-based drug loading in SCLs and hydrogel materials [9].

2.5. Drug release

The *in vitro* release profiles of the hydrogels were evaluated under sink conditions over 72 h. Following SCI, drug-loaded samples (n = 4) were weighed, immersed in 3 mL PBS, and incubated at 37 °C with agitation (180 rpm). For conventionally impregnated samples, the samples were first removed from the soaking solution and lightly blotted before immersion in PBS. During the initial 8 h, 200 μL aliquots were withdrawn at predetermined intervals and immediately replaced with fresh PBS. Subsequent samples were collected at 24 h, 48 h, and 72 h following the same procedure. TA concentrations in the release medium were determined by UV–Vis spectrophotometry (Multiskan GO, Thermo Scientific, UK) at 239 nm, using a rigorously obtained calibration curve (0–20 μg.mL^{-1}). After completion of the release study, the hydrogels (n = 4) were rinsed and transferred to glass vials containing 3 mL methanol to extract the remaining drug. After 24 h, the TA concentration in the methanol extracts was determined by measuring the solutions absorbance at 249 nm using a new calibration curve with methanol (0–45 μg.mL^{-1}). The methanol was replaced completely, and extraction continued until no further TA was detected. The cumulative amount of TA released *in vitro* plus the total extracted with methanol yielded the overall amount of drug loaded in each sample.

2.6. Physico-chemical properties

To assess the suitability of hydrogels treated with supercritical CO_2 ($scCO_2$) for use as SCL materials, an extensive physico-chemical characterisation of their properties was conducted. Both non-treated (NT) samples and those exhibiting the most effective TA release following $scCO_2$ processing were evaluated.

2.6.1. Equilibrium water content and swelling ratio

The swelling ratio (SR) of the SCLs materials in DD water and PBS

Table 1
Experimental design matrix generated by FFD of the four independent parameters for impregnation of TA in SCLs. The operational temperature and pressure values were maintained within ± 0.1 ºC and ± 0.5 bar, respectively.

Samples	Independent variables			
	Time of impregnation (h)	**Pressure** (bar)	**Temperature** (°C)	**Co-solvent** (% v/v)
SCI_t2_P200_T40_C0	2	200	40	0
SCI_t2_P200_T40_C5	2	200	40	5
SCI_t2_P200_T60_C0	2	200	60	0
SCI_t2_P200_T60_C5	2	200	60	5
SCI_t2_P300_T40_C0	2	300	40	0
SCI_t2_P300_T40_C5	2	300	40	5
SCI_t2_P300_T60_C0	2	300	60	0
SCI_t2_P300_T60_C5	2	300	60	5
SCI_t4_P250_T50_C2.5	4	250	50	2.5
SCI_t6_P200_T40_C0	6	200	40	0
SCI_t6_P200_T40_C5	6	200	40	5
SCI_t6_P200_T60_C0	6	200	60	0
SCI_t6_P200_T60_C5	6	200	60	5
SCI_t6_P300_T40_C0	6	300	40	0
SCI_t6_P300_T40_C5	6	300	40	5
SCI_t6_P300_T60_C0	6	300	60	0
SCI_t6_P300_T60_C5	6	300	60	5

was calculated according to Eq. 1. For each system, the dried hydrogel discs (n = 3) were weighed (W_d) and individually immersed in 3 mL of the corresponding solution, at RT. The NT samples were first dried for 24 h at 40 ºC, whereas $scCO_2$-treated samples were already in a dry state. Once equilibrium swelling was reached (≈24 h after), the hydrated samples were removed, gently blotted with absorbent paper, and weighed (W_h). The equilibrium water content (EWC) was also calculated through Eq. 2, using the same values.

$$SR\ (\%) = \frac{W_h - W_d}{W_d} \times 100 \quad (1)$$

$$EWC\ (\%) = \frac{W_h - W_d}{W_h} \times 100 \quad (2)$$

2.6.2. Light transmittance and refractive index

To evaluate the optical transparency of the hydrogels, light transmittance was measured following the 24 h swelling period in DD water and in PBS. Each sample was carefully blotted to remove excess surface moisture and mounted on the inner front face of a quartz cuvette. Transmittance was determined from absorbance values obtained using a UV–Vis spectrophotometer, across the 200–700 nm wavelength range, using 1 nm scanning intervals.

The refractive index of the swollen SCL materials (after 24 h hydration in DD water and PBS) was measured using an Abbe refractometer (AR4, KRUSS, Germany) at 589.6 nm and RT.

All measurements were carried out in triplicate for each formulation.

2.6.3. Wettability

The water contact angle (CA) of the hydrated hydrogels was measured using the captive bubble method. Rectangular samples (area of 3 cm^2) were glued to a metallic support and inserted in a liquid cell filled with DD water at RT. Air bubbles were placed underneath the sample, eight images were taken over 30 s at predetermined time intervals using a video camera (CV-A50, JAI, Spain) attached to a microscope (Leica MZ6, Leica Microsystems, Germany). The images were analysed with the Axisymmetric Drop Shape Analysis (ADSA) software. Five bubbles were formed for each system.

2.6.4. Thermotropic properties

The thermotropic properties of the hydrogels, both before and after $scCO_2$ treatment, were investigated using a differential scanning calorimeter (DSC 200 F3 Maia, NETZSCH, Bremen, Germany) to identify any changes phase induced by the treatment. Hydrogel samples with a diameter of 3 mm were analysed in both hydrated and dry states. For dry state analysis, $scCO_2$-treated samples were tested immediately after processing, while untreated samples were previously dried in a vacuum oven at 36 °C for 72 h. For hydrated state analysis, samples were immersed in DD water for 24 h, gently blotted to remove surface moisture, and then placed in the crucibles for testing. Thermal measurements were performed using a heat–cool–heat cycle, with heating and cooling rates of 10 °C·min^{-1} . The temperature range was 25–250 °C for dry samples and −45 °C to 40 °C for hydrated samples. Three independent measurements were conducted for each condition. Thermograms were analysed using NETZSCH Proteus Thermal Analysis software, and the fusion enthalpy (ΔH_{fus}) was determined from the area under the peaks corresponding to the first heating cycle.

2.6.5. Morphology

The materials morphology was evaluated by scanning electron microscopy (SEM, Phenom Prox G6 Desktop SEM, ThermoScientific, Waltham, Massachusetts, EUA). Prior to the analysis, the samples hydrated in DD water were first frozen at −20ºC, lyophilised overnight and then coated with an electrically conductive material layer (Au:Pd, 20:80) in an automatic turbomolecular pumped sputter coater (Q150T ES, Quorum Technologies, UK). Several images at magnifications of 500x, 1000x and 3500x were taken, at a low accelerating voltage of 10 kV to prevent thermal damage and minimise charging of the delicate polymer surface.

2.6.6. Chemical structure

The chemical structure of the hydrogels and their constituent monomers was analysed using Fourier Transform Infrared Spectroscopy (FTIR). The measurements were performed with a Spectrum Two FT-IR spectrometer (PerkinElmer®, USA), equipped with a diamond ATR crystal accessory, over a wavenumber range of 4000–400 cm^{-1} with a resolution of 1 cm^{-1}. Dried hydrogel discs (11 mm diameter) were used for the analysis. During FTIR acquisition, the applied pressure was manually controlled to ensure proper contact between the sample and the crystal. Transmittance spectra were normalised using GraphPad® Prism 10.1.0 (GraphPad Software, USA), by setting 0% and 100% baselines to the minimum and maximum transmittance values, respectively. Normalisation was achieved by dividing each transmittance value by the maximum value for that sample. Measurements were performed in triplicate for each hydrogel formulation.

2.7. Biocompatibility tests

For the biocompatibility assays TA-loaded samples were sterilised by autoclaving in drug-loading solution (TA, 1 mg.mL^{-1} in PBS, 1 mL/disc), while unloaded samples were sterilised in the same volume of DD water. Sterilisation was performed in closed vials (MLS−3020, SANYO Electric Co. Ltd., Japan) at 121ºC for 20 min.

2.7.1. Irritability assay

The Hen's Egg Test on the chorioallantoic membrane (HET-CAM) is a simple, cost-effective, and valuable alternative method used to predict ocular irritability of devices before pre-clinical testing. The assay was conducted in accordance with the Interagency Coordinating Committee on the Validation of Alternative Methods (ICCVAM) guidelines [34].

Fertilised hen's eggs were obtained from Sociedade Agrícola da Quinta da Freiria (Portugal) and incubated for eight days at 37.0 ± 0.7 °C and 60 ± 4% relative humidity using an HHD incubator (model YZ−56S, China). On day 9, a rotary saw (Dremel 3000, Breda, Netherlands) was used to carefully open the eggshell at the air cell located at the larger end of the egg. The removed shell segment exposed the inner membrane, which was hydrated with a few drops of 0.9% NaCl solution. The eggs were then returned to the incubator for an additional 5 min. Following this period, the inner membrane was gently removed to expose the CAM. Hydrogel discs (6 mm diameter) were placed directly onto the CAM and monitored for 5 min to assess the occurrence of any acute reactions. The irritation potential of the hydrogels was quantified using the irritation score (IS, Eq. 3) that considers the time (in seconds) until the onset of haemorrhage (t_h), vascular lysis (t_{vl}), and coagulation (t_c). Based on the IS the samples were classified as non-irritation (IS: 0 – 0.9), slightly irritant (IS: 1 – 4.9), moderately irritant (IS: 5 – 8.9) or severely irritant (IS: 9 – 21) [35].

$$\textit{Irritation score}\ (IS) = \left[5 \times \left(\frac{301 - t_h}{300}\right) + 7 \times \left(\frac{301 - t_{vl}}{300}\right) + 9 \times \left(\frac{301 - t_c}{300}\right)\right] \quad (3)$$

As controls, 300 μL of 0.1 M NaOH (positive control) and 0.9% NaCl (negative control) were applied directly to the CAM surface. All experiments were performed in triplicate.

2.7.2. Cell viability

Cell viability was evaluated using a cytotoxicity assay to determine whether the sterilised hydrogel formulations and/or the drug released from them led to any toxic effects on NIH/3T3 fibroblast cells. The assay was conducted under sterile conditions in a vertical laminar flow cabinet (Mars Safety Class 2, Scanlaf, Allerød, Denmark) in accordance with ISO 10993–5: Biological evaluation of medical devices – Part 5: Tests for in vitro cytotoxicity [36].

Cells were seeded in DMEM into 96-well plates at a density of 1×10^4 cells/well and incubated for 24 h at 37 °C in a humidified atmosphere containing 5% CO_2. Samples discs (6 mm) were also incubated in DMEM at the same conditions than the cells. The hydrogels extraction ratio was defined following the ISO 10993–12:2012 [36]. Following incubation, the medium was replaced with hydrogels extracts. Instead, fresh DMEM was added for the negative control, and DMEM containing 10% DMSO was used as the positive control. Plates were incubated for an additional 24 h under the same conditions.

After incubation, cell morphology and possible detachment were visually assessed and documented via microscopy. The medium was then removed, the cells were washed with PBS and MTT solution (0.5 mg.mL^{-1} in serum-free DMEM) was added to each well, followed by incubation for 3 h under the same conditions. Subsequently, MTT solvent (0.1% v/v IGEPAL in isopropanol with 4 mM HCl) was added to each well, followed by orbital shaking for 1 h at room temperature to solubilise the formazan crystals. Finally, absorbance was measured at 565 nm using a microplate reader (Infinite 200Pro, Tecan). Cell viability was calculated relative to the negative control. All samples were tested in quintuplicate.

2.8. Statistical analysis

Quantitative data are expressed as mean ± standard deviations (SD). The statistical analysis was conducted using GraphPad® Prism 10.1.0 software (GraphPad Software, USA). Data normality was checked using the Shapiro-Wilk test. For normally distributed data, a one-way analysis of variance (ANOVA) was performed, followed by a post-hoc Tukey test to determine statistical significance among multiple data sets. For non-parametric data, the Kruskal-Wallis test was used followed by Dunn's multiple comparisons tests. Statistical significance were defined at $p < 0.05$ (*), $p < 0.01$ (**), $p < 0.001$ (***) and $p < 0.0001$ (****), with a 95% confidence interval. The 2-level factorial design batches were analysed statistically using multiple regression analysis and ANOVA with Design Expert® 13.0 software by Stat-Ease Inc., located in Minneapolis, MN.

3. Results and discussion

3.1. Preliminary analysis of the $scCO_2$ influence on the produced SCLs materials

No foaming phenomenon was observed in the samples that underwent the SCT during the preliminary experiments for the SCI method implementation (Figure S1, Supplementary Information). Samples treated at both extreme pressures and temperatures in the presence or absence of a co-solvent did not show any visual alterations showing high transparency. Foaming in polymers is commonly reported in literature under specific depressurisation conditions, when rapid desorption of a gaseous phase from the polymer matrix occurs [37], suggesting that the employed depressurisation rates of 0.1–2 bar.min^{-1} were appropriate for the experiments conducted. In addition, the diameter and thickness of $scCO_2$ treated samples remained the same, meaning that the plasticisation effect was reversible.

3.2. TA impregnation and release from SCLs material

3.2.1. TA Impregnation Efficiency

The drug loading capacity of the NT and SCI samples was evaluated as one of the principal response variable dictating system performance. Concerning the system TA/$scCO_2$ Sodeifan *et al.* [30] reported solubility data of TA in $scCO_2$ at temperatures from 308 to 3338 K and pressure up to 270 bar, with values ranging from 3.15×10^{-5} to 2.30×10^{-4} (mole fraction). The reported data showed that the SCI system used in this work was bellow saturation conditions, since the mole fraction of TA in the supercritical fluid, ranged from 1.14×10^{-5} to 1.30×10^{-5} (mole fraction). This ensures that the TA inside the vessel could be completely solubilised by $scCO_2$. Additionally, since after each experiment it was found that TA was still available in the thimble and that the amount of impregnated TA, in each experiment, was well below that placed inside the impregnation vessel at the beginning of the run, it can be inferred that the proposed system was adequate to the planned study. As shown in Fig. 2, the SCI parameters, i.e. pressure, temperature, time, and co-solvent content, significantly influenced the total amount of TA loaded into the hydrogel matrix. It can be observed that higher pressure and temperature result in a superior amount of drug loaded. Concerning the time of impregnation and presence of co-solvent, although in general the same tendency was found, in a few cases an inverse correlation was observed.

Regarding the effect of pressure, at constant temperature, it was observed that the amount of drug loaded increased with pressure. However, the observed trend is not the result of the well-established relation of solubility increase with pressure due to increase in solvent

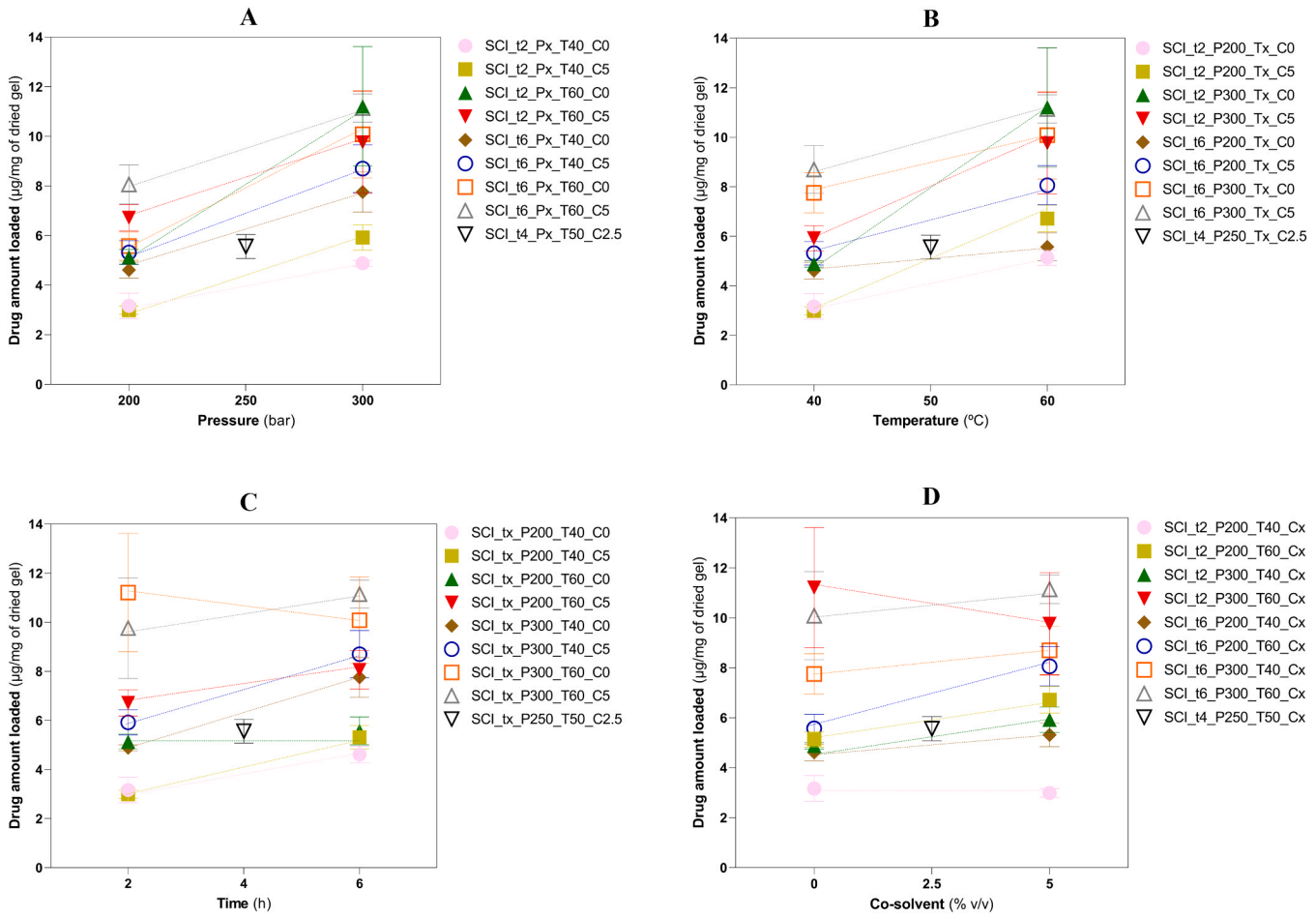

Fig. 2. Influence of a) pressure, b) temperature, c) impregnation time and d) co-solvent on the total amount loaded of TA loaded. The error bars are the ± standard deviations (n = 4). NT_TA_ (time of impregnation): samples prepared by conventional impregnation method; SCI samples name follow the description in Table 1. The 'x' in the sample names denotes the value of the variable plotted on the x-axis. Both amounts are expressed in µg of drug per mg of dried gel.

density [23,24,31], since the amount of TA in the impregnation high-pressure vessel is bellow TA's saturation solubility in $scCO_2$, thus resulting that the fluid phase is able dissolve the entire solute, resulting that the system will not be solubility-limited. Moreover, raising pressure increases $scCO_2$ density (and thus increases the total amount of CO_2 present in the high pressure vessel), but if the total dissolved TA mass is essentially fixed, its concentration (expressed as mass fraction = $mass_{TA}/(mass_{scCO2}+mass_{TA})$ can even decrease with pressure as $mass_{scCO2}$ increases. Therefore, the observed increase in the amount of drug loaded with pressure is possibly more consistently due to pressure-induced changes in the drug–polymer–CO_2 partitioning equilibrium and by enhanced CO_2 sorption into the polymer, which promotes swelling and plasticisation (increased free volume and segmental mobility), thereby facilitating drug diffusion into the matrix and increasing the polymer's effective capacity to retain solute during and after depressurisation [38–40]. In situ measurements carried out by Champeau *et al.* [38] showed that CO_2 uptake and polymer swelling can evolve together with drug uptake during impregnation, reinforcing the view that pressure primarily acts by modifying the polymer's physical/thermodynamic state under CO_2 and the resulting partitioning, rather than merely by increasing solvent power. Additionally, recent CO_2 sorption/diffusion studies in polymers [41] confirm that, at constant temperature, equilibrium CO_2 uptake increases with pressure, supporting the role of pressure in strengthening plasticisation/swelling effects that can enhance impregnation. Furthermore, although $scCO_2$ solubility is generally correlated with density/pressure, those relations are most relevant near saturation [42] and thus since TA is expected to be fully dissolved in $scCO_2$, at the experimental conditions used in this work, the pressure effects should possibly be due to partitioning and polymer swelling/plasticisation. It was found that $scCO_2$ presents a considerable increase of diffusivity with temperature for polymeric systems as HEMA [43,44], which reinforces the idea that supercritical impregnation can benefit from increased temperature. Also, time consequently impacts the drug diffusion and its penetration into the material: a longer contact time is expected to improve the impregnation yield, passing from a surface to a more in-depth process. Data from literature show that longer impregnation times usually have a positive influence on the increase of total impregnated quantity [45,46]. Finally, regarding the effect of the co-solvent, its presence can either increase or decrease drug loading depending on the temperature–pressure conditions. This is due to competing effects shift with these parameters: co-solvent raises drug solubility in $scCO_2$ (favouring uptake) but can also change the thermodynamic properties altering the extraction selectivity, perturb polymer–CO_2 phase behaviour, swelling/plasticisation, and drug–polymer partitioning, reducing the drug loading. The net outcome depends on the balance of these effects at each temperature–pressure–time combination. This issue is discussed by several authors that also found ambiguous results [46–48].

3.2.2. *TA release profiles*

The TA release profiles from all SCI samples are shown in Fig. 3. For comparative purposes, the results obtained with samples prepared by simple soaking in TA solution for 2 h, 4 h, 6 h and 72 h are also presented. Table 2 presents the values of the cumulative amount of drug

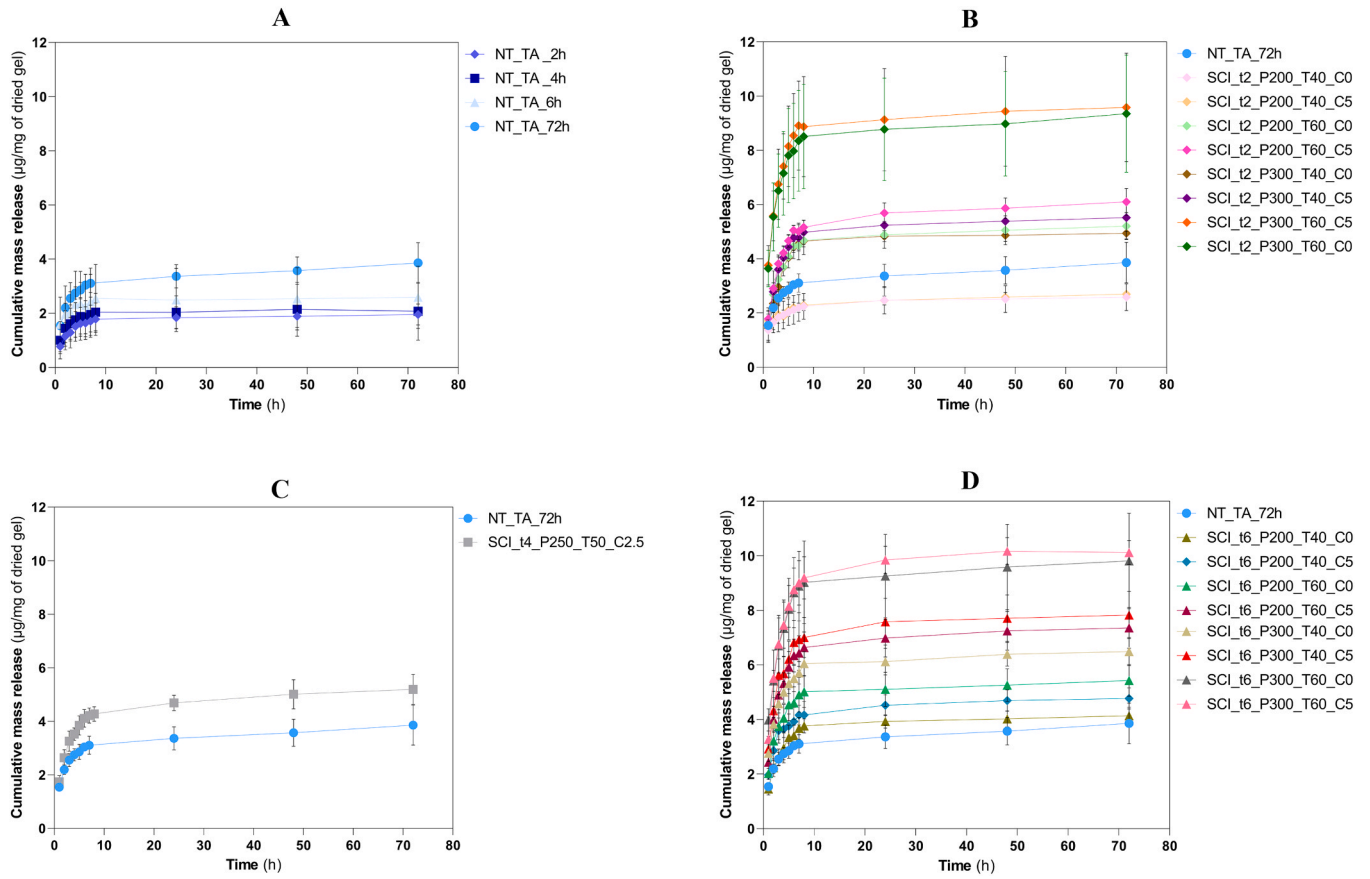

Fig. 3. Cumulative release profiles from TA-loaded hydrogels prepared with different drug loading times. a) through the conventional method, b) by SCI 2 h, c) by SCI 4 h and d) by SCI 6 h. For comparative purposes the profile NT_TA_72 h is shown in all figures. The error bars are the ± standard deviations (n = 4). NT_TA_ (time of impregnation): samples prepared by conventional impregnation method; SCI samples name follow the description in Table 1.

released after 72 h, the total amount of drug loaded, and the percentage of drug released relatively to the loaded. The respective comparative statistical analysis is shown in Table S1A and Table S1B, in Supplementary Information.

Considering the NT samples (Fig. 3A), it can be seen that the increase of the impregnation time led to an increase in the amount of TA released from the samples, being more pronounced for the hydrogel loaded for 72 h. This was expected, considering results found in the literature for other systems [49]. At the 72 h time point, the amount of TA released from hydrogels soaked for 72 h was 49%, 86% and 98% higher compared to those soaked for 6 h, 4 h and 2 h, respectively (Table 2). However, the differences between the release curves for the shorter impregnation times (2 h, 4 h and 6 h), were not statistically significant. Regarding the release kinetics, a sustained TA release was observed for the first 8 h (Fig. 3). Still, the kinetics of the NT_TA_72 h slightly differs from the remaining NT samples, as the release of TA for longer times still increases, although at a lower rate. Such result may derive from the significant amount of TA that still remains in the hydrogel matrix. Since the NT_TA_72h system exhibited the best release profile among the NT samples studied, it was henceforth designated as the reference system for comparison with SCI samples.

The results suggest that almost all SCI samples showed a successful impregnation, demonstrating a significant increase in the amount of TA released when compared to conventional impregnation (NT_TA_72h). Moreover, the percentage of drug released from the SCI samples (between 81.1% and 99.2%) is considerably higher than that observed for NT_TA_72h (29.7%), demonstrating the high efficiency of the process. SCI_t2_P200_T40_C0 and SCI_t2_P200_T40_C5 (Fig. 3B) were the only systems that presented lower amounts of drug released comparatively to the reference system (NT_TA_72h). These values were similar to the one found with 6 h of conventional impregnation.

In absolute terms, the best performing systems were SCI_t6_P300_T60_C5, SCI_t6_P300_T60_C0, SCI_t2_P300_T60_C5 and SCI_t2_P300_T60_C0, since they led to cumulative drug releases superior to 9 µg TA per mg of dried gel, significantly higher than the observed for the remaining systems. These four systems share the distinction of being the only ones combining high pressure (300 bar) and high temperature (60 ºC) in the processing parameters, although they present distinct impregnation times (2 h or 6 h) and co-solvent concentrations (0%v/v or 5%v/v).

3.2.3. *Statistical analysis of TA impregnation and release*

The isolated evaluation of the effects of individual experimental parameters on the response variables cumulative drug release at 72 h (Y1) and total amount of drug loaded (Y2) is not sufficient to fully understand the system's overall behaviour. The effect of the interaction between the experimental factors on the response variables must also be accounted. The statistical analysis of the experimental design matrix enables the identification of both the main effects and the interactions that significantly impact the response variables. The detailed study to assess these effects was the performed using DoE software (Design-Expert®).

Table 2
TA cumulative mass released values, total amount of drug contained in the conventionally loaded and SCI SCLs materials and percentage of drug released. The error corresponds to the standard deviation (n = 4). NT_TA_ (time of impregnation): samples prepared by conventional impregnation method; SCI samples name follow the description in Table 1. Both amounts are expressed in μg of drug per mg of dried gel.

Samples	Response variables		Percentage of drug released (%)
	Y1: Cumulative drug released at 72 h ($\mu g.mg^{-1}$)	Y2: Drug amount loaded ($\mu g.mg^{-1}$)	
NT_TA_2h	1.95 ± 0.38	2.86 ± 1.04	68.2
NT_TA _4h	2.07 ± 1.06	2.70 ± 0.36	76.7
NT_TA_6h	2.59 ± 1.14	3.48 ± 1.29	74.4
NT_TA_72h	3.86 ± 0.75	13.01 ± 3.03	29.7
SCI_t2_P200_T40_C0	2.59 ± 0.50	3.17 ± 0.45	81.7
SCI_t2_P200_T40_C5	2.69 ± 0.15	2.97 ± 0.17	90.7
SCI_t2_P200_T60_C0	5.20 ± 0.49	5.36 ± 0.30	97.0
SCI_t2_P200_T60_C5	6.10 ± 0.50	6.72 ± 0.53	90.7
SCI_t2_P300_T40_C0	4.94 ± 0.21	4.98 ± 0.13	99.2
SCI_t2_P300_T40_C5	5.51 ± 0.51	5.92 ± 0.51	93.1
SCI_t2_P300_T60_C0	9.35 ± 0.43	11.21 ± 2.41	83.4
SCI_t2_P300_T60_C5	9.58 ± 2.00	9.76 ± 1.78	98.2
SCI_t4_P250_T50_C2.5	5.19 ± 0.56	5.56 ± 0.48	93.5
SCI_t6_P200_T40_C0	4.14 ± 0.31	4.61 ± 0.33	89.8
SCI_t6_P200_T40_C5	4.77 ± 0.39	5.32 ± 0.48	89.7
SCI_t6_P200_T60_C0	5.43 ± 0.58	5.57 ± 0.57	97.5
SCI_t6_P200_T60_C5	7.35 ± 0.75	8.06 ± 0.79	91.2
SCI_t6_P300_T40_C0	6.48 ± 0.51	7.76 ± 0.81	83.5
SCI_t6_P300_T40_C5	7.83 ± 0.86	8.69 ± 0.96	90.1
SCI_t6_P300_T60_C0	9.81 ± 1.75	10.08 ± 1.77	97.3
SCI_t6_P300_T60_C5	10.12 ± 0.44	11.14 ± 0.57	90.8

In a first step, the adequacy and validity of the proposed experimental design was evaluated through the analysis of degrees of freedom for lack of fit and pure error, as well as the power of the design model and the correlation matrix of the design, being verified that the design can adequately be used to determine the effect of the experimental factors on the response variables. In the Supplementary Information section is described the performed evaluation.

A first order fractional model (Eq. 4) was used to fit the experimental results. The general equation includes up to four-factor interaction parameters, which, in the course of the statistical evaluation, may be considered insignificant, and as such, the model may be reduced to a lower factor's interactions order.

$$Y = \beta_0 + k_1X_A + k_2X_B + k_3X_C + k_4X_D + k_{1,2}X_1X_2 + k_{1,3}X_1X_3 + k_{1,4}X_1X_4 + k_{2,3}X_2X_3 + k_{2,4}X_2X_4 + k_{3,4}X_3X_4 + k_{1,2,3}X_1X_2X_3 + k_{1,2,4}X_1X_2X_4 + k_{1,3,4}X_1X_3X_4 + k_{2,3,4}X_2X_3X_4 + k_{1,2,3,4}X_1X_2X_3X_4 \quad (4)$$

Concerning Eq. 4, Y is the response variable (Y_1: cumulative drug release and Y_2: drug amount loaded), $X_{A\text{-}D}$ is the experimental factor (X_A – Time of impregnation, X_B – Pressure, X_C – temperature and X_D – %v/v of co-solvent), k_i (with i:1–4) are the linear coefficients, k_{ij} ($k_{1,2}$, $k_{1,3}$, $k_{1,4}$, $k_{2,3}$… to $k_{3,4}$) are the two-factor interaction coefficients, $k_{1,2,3}$ to $k_{2,34}$ the three-factor interaction coefficients and k_{1234} the four-factor interaction coefficient.

The statistical analysis of each response was carried out through analysis of variance (ANOVA) aiming to evaluate the statistical significance of the model. Values of Prob> F less than 0.05 ($p < 0.05$) indicate that the model terms are significant.

Tables 3 and 4 present the analysis of variance (ANOVA) for each of the response variables: cumulative drug release at 72 h (Y1) and drug amount loaded (Y2), respectively. These tables show the p-values associated with each individual model term. The 'Term' column in each table presents the main effects and the interactions parameters.

A brief overview of the results presented in these tables show that for both responses all of the main experimental factors showed significant effect on both response variables, though pressure and temperature had the most significant effect by virtue of the highest amount of the Fisher value (F-value) as well as the lowest p-value ($p < 0.0001$). Conversely, only two of the interactions parameters: impregnation time/temperature and pressure/temperature showed significant effect on the response variables, confirmed by the p-value < 0.05. However, the effect these two interaction parameters was lower than that of the main experimental factors with low significance: i.e. time of impregnation and co-solvent (%v/v). Additionally, the three-factor interaction temperature/pressure/co-solvent also presented significance and was therefore considered for the model. The Fit statistics of the ANOVA analysis for the two responses are summarised in Table S3 (see Supplementary Information section). For the Y1 response: cumulative drug release at 72 h, the statistical analysis of the ANOVA results showed a coefficient of determination (R^2) of 0.9556, an adjusted coefficient of determination ($R^2_{Adjusted}$) of 0.9298 and a predictive coefficient of determination ($R^2_{Predicted}$) of 0.8910. Concerning response variable Y2 (drug amount loaded), values of 0.9424, 0.9088 and 0.8248 were obtained for the coefficients R^2, adjusted R^2 and predicted R^2, respectively. Adjusted R^2 accounts for the effect of the number of predictors (coefficients) in the proposed model (i.e. the inclusion of unnecessary parameters in the model will be penalising, decreasing this coefficient value) and predictive R^2 assesses how well the model predicts new data outside the design space. A difference less than 0.2 between these coefficients shows a good agreement, indicating a well-balanced and not over-fitted model, which was observed for both responses, meaning that the proposed models can reliable predict the responses for a new data range.

The PRESS (predicted residual sum of squares) parameters, for both responses, present a low value, indicating higher predictive accuracy and robustness of the models. Note that, statistically PRESS is the square sum of the residual differences between actual response values and model predicted response values (i.e. PRESS is the overall prediction error for new data) and thus smaller values of PRESS indicate a more robust and stronger predictive model. Furthermore, the lack of fit test result (degree of freedom = 8 > 3) also shows that the model fits well across the studied factor range, as it was not statistically significant.

The regression model based on the actual values of the experimental factors lead to the following first degree three-factors interaction

Table 3
Analysis of variance (ANOVA) for response variable Y1: (drug release at 72 h) in actual units for response surface fractional three-factor interaction model.

Term	SS[a)]	df	MS[b)]	F- value	p-value	Remarks
Model	99.74	7	14.25	36.93	< 0.0001	Significant
X_A - impregnation time	8.40	1	8.40	21.78	0.0005	Significant
X_B - Pressure	40.54	1	40.54	105.07	< 0.0001	Significant
X_C - Temperature	43.20	1	43.20	111.97	< 0.0001	Significant
X_D - %v/v co-solvent	4.22	1	4.22	10.94	0.0063	Significant
X_{AC}	3.22	1	3.22	8.34	0.0136	Significant
X_{BC}	2.51	1	2.51	6.51	0.0254	Significant
X_{BCD}	1.94	1	1.94	5.03	0.0446	Significant
Lack of Fit	0.9503	8	0.1188	0.1291	0.9926	Not significant

a) sum of squares, b) sum of mean squares

Table 4
Analysis of variance (ANOVA) for response variable Y2: (drug loaded amount) in actual units for response surface fractional three-factor interaction model.

Term	SS[a)]	df	MS[b)]	F- value	p-value	Remarks
Model	115.85	7	16.55	28.03	< 0.0001	Significant
X_A - impregnation time	11.30	11	11.30	19.15	0.0009	Significant
X_B - Pressure	47.72	1	47.72	80.84	< 0.0001	Significant
X_C - Temperature	46.01	1	46.01	77.93	< 0.0001	Significant
X_D - %v/v co-solvent	3.52	1	3.52	5.96	0.0311	Significant
X_{AC}	5.65	1	5.65	9.56	0.0093	Significant
X_{BC}	2.90	1	2.90	4.91	0.0467	Significant
X_{BCD}	3.24	1	3.24	5.035.49	0.0371	Significant
Lack of Fit	4.27	8	0.5338	0.7587	0.6592	Not significant

a) sum of squares b) sum of mean squares

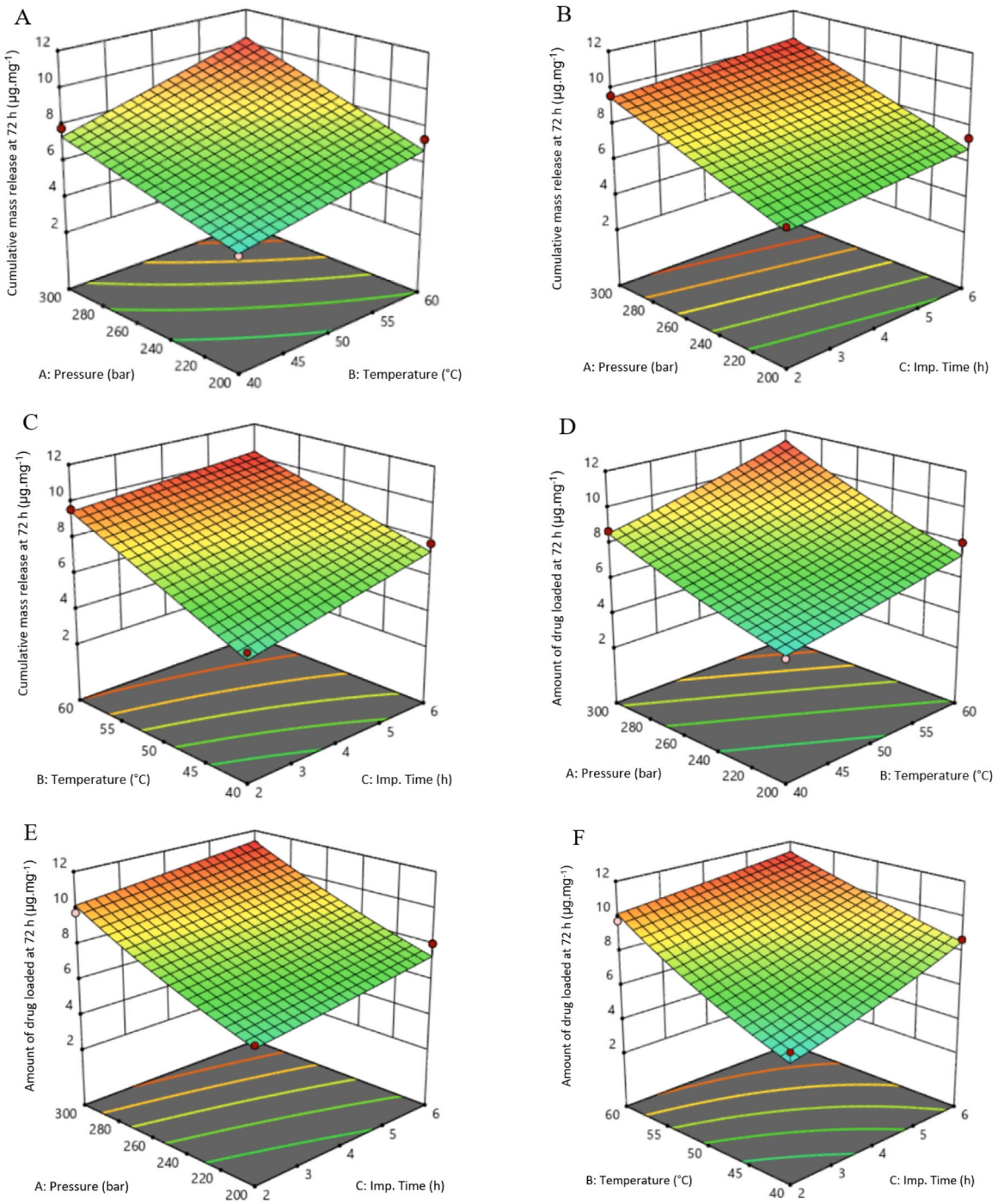

Fig. 4. Factorial surface response plots for Y1 – cumulative drug released at 72 h (A, B, C) and Y2 – drug amount loaded (D, E, F).

factorial equations, Eqs. 5 and 6, for the Y1 and Y2 response variables, respectively:

- cumulative drug release at 72 h:

$$Y1 \quad (\mu g \bullet mg^{-1}) = -5.7245 + 1.49018 \times X_A - 0.010422 \times X_B + 0.044366 \times X_C + 0.304481 \times X_D - 0.022894 \times X_A X_B + 0.000835 \times X_B X_C - 7.70212 \times 10^{-6} \times X_A X_B X_C \quad (5)$$

drug loaded amount:

$$Y2 \quad (\mu g \bullet mg^{-1}) = -7.03842 + 1.91343 \times X_A - 0.011412 \times X_B + 0.060967 \times X_C + 0.397311 \times X_D - 0.030254 \times X_A X_B + 0.000928 \times X_B X_C - 0.000016 \times X_A X_B X_C \quad (6)$$

being each experimental factor X_i in the actual value: X_A – impregnation time (min), X_B – pressure (bar), X_C – temperature (ºC) and X_D – %v/v of co-solvent.

The obtained results of ANOVA DoE show the importance of the experimental factors: pressure and temperature in the response variables, which was already inferred from the initial analysis of the experimental results. Temperature presents a positive influence on each of the responses, meaning an increase of the response with the increase of temperature, but pressure shows a negative influence on the responses. Also, the %v/v of co-solvent was the experimental factor with less significance, in accordance to the preview analysis of the experimental results. Additionally, the 2-factors interaction: time of impregnation·temperature and temperature·pressure were the only interaction parameters with significance, presenting a positive effect on the response variables.

Nevertheless, the overall ANOVA analysis results suggest that the behaviour and interactions observed are consistent for both responses, reinforcing the robustness of the findings across multiple response variables.

The obtained models for each response variable were used to obtain a 3D- representation graphic of the response surfaces that depicted the predicted response as a function of the most significant three-factors interaction parameters, in all the design domain studied, and considering the other independent factors constant (i.e. 3D-representation of Y1 and Y2 as function of time of impregnation and temperature, as function of time of impregnation and pressure, and as a function of pressure and temperature). Fig. 4, presents this 3-D graphic representation.

The 3D plots reveal that factor interactions align closely with the response trends already discussed, allowing the identification of the region where the response achieves optimal levels. For the release response the most significant experimental factors were pressure and temperature and also, although in a less extension, the impregnation time. Likewise, for the loaded drug response the same experimental factors revealed to be significant.

The numerical optimisation of the experimental factors was carried out using Design-Expert® software, with the aim of determining the values of experimental factors, within the range of the design space that would maximise the response variables.

The software uses *Desirability* as the objective function in optimisation. The objective function ranges between zero (outside of the limits) to one (at the goal), with higher scores indicating better outcomes, helping to identify the best compromise settings across all factors. When analysing the optimisation and desirability with Design-Expert®, desirability indexes indicate that the selected factor ranges are appropriate to identify the region where the response is maximised. The contour graphical representation (iso-response lines) of the desirability indexes is shown in Figure S2 (see supplementary Information section) as well as the contour graphics showing the iso-response results for each response variable as a function of pressure and temperature (Figure S3).

Based on the results described above, the SCI hydrogels expected to guarantee the highest drug loading and a higher release of TA, are those whose impregnation was performed during 6 h at 300 bar and 60 °C with (SCI_t6_P300_T60_C5) or without (SCI_t6_P300_T60_C0) co-solvent, and those with the same operational pressure and temperature but with a contact time of 2 h (SCI_t2_P300_T60_C5 and SCI_t2_P300_T60_C0). Since, the co-solvent effect was considered negligible has it had almost no effect on the impregnation efficiency, the operational conditions of SCI_t2_P300_T60_C0 and SCI_t6_P300_T60_C0, were selected as the best conditions for the SCI of the developed TA-eluting SCLs materials. For comparison purposes, hydrogels were submitted to a SCT in the absence of drug and designated has follows: SCI_t2_P300_T60_C0-ND (60 °C, 300 bar, 2 h) and SCI_t6_P300_T60_C0-ND (60 °C, 300 bar, 6 h). Samples not submitted to SCT, unloaded (NT) and TA loaded (NT_TA_72h) were also tested to evaluate the SCI efficacy.

3.3. Hydrogel characterisation

The hydrogels were first characterised without the incorporation of any drug. This allowed to establish a clear understanding of their base physical, thermal, and morphological properties. This initial characterisation was essential for evaluating the materials' suitability to be used in SCLs.

The SR of the samples in DD water and PBS is reported in Table 5. Statistical analysis, conducted employing one-way ANOVA and Tukey's multiple comparisons test, revealed no statistically significant differences ($p > 0.05$) across all comparisons.

Results show that the $scCO_2$ had a negligible effect on the SR of the hydrogel samples in DD water, being in line with what is reported in literature [23]. Comparing the results of DD water to the ones of PBS, almost no effect of the ionic strength of the PBS liquid media was observed on the swelling behaviour, suggesting that the polymeric network is essentially non-ionic [31]. A similar pattern was found for the ability of the hydrogel to bind water in its equilibrium state. The EWC values of the samples did not show any statistically significant effect related to the SCT. These values are close to those reported by Tran and Yang *et al.* [50] who refer values of 44.5 ± 1.1% for a similar SCL's material formulation with the same proportion of TRIS. These values are not particularly high since approximately 40% of the hydrogel's total dry weight arises from the hydrophobic TRIS. This undermines the contribution of the hydrophilic monomers used in the production of the hydrogel matrix that usually improve wearer comfort [51]. Still, the obtained values in this work are within those reported for commercially available SCLs that display a wide range of EWC, from 24% to 79%, indicating that the produced materials fulfil this criterium [52,53].

The effect of SCT on the light transmittance of the material is also presented in Table 3. Both treated and untreated hydrogel samples presented a light transmittance > 90% in the visible light range (400 – 700 nm), either hydrated in DD water and in PBS. These observations were in agreement with previous studies where SCI was performed without compromising the optical transparency [23]. Overall, the obtained results support the applicability of these materials in SCLs [54].

Regarding the refraction indices of the samples (Table 5), the data does not show any statistical difference when comparing the SCT and NT materials. It is important to mention that these values are similar to the one of the cornea, i.e., 1.376 [54] and that they fall within the nominal refractive index range stated for commercially available SCLs (1.374 – 1.426) [55]. Additionally, similar results for SCLs were reported in the literature for similar materials [56].

In terms of CA (Table 5), no statistical significance was observed between NT and SCI_t6_P300_T60_C0-ND ($p = 0.4202$). However, SCI_t2_P300_T60_C0-ND presented a value slightly lower when compared to NT ($p < 0.0001$) and SCI_t6_P300_T60_C0-ND

Table 5
Characterisation results of NT, SCI_t2_P300_T60_C0-ND and SCI_t6_P300_T60_C0-ND. The error bars are the ± standard deviations (n = 4).

Property		Samples		
		NT	SCI_t2_P300_T60_C0-ND	SCI_t6_P300_T60_C0-ND
SR (%)	DD water	68.9 ± 0.8	68.1 ± 1.6	68.9 ± 4.6
	PBS	68.1 ± 2.0	69.3 ± 3.2	67.1 ± 3.3
EWC (%)	DD water	40.8 ± 0.3	40.8 ± 1.6	40.1 ± 0.5
Transmittance (%) (400–700 nm)	DD water	99.1 ± 0.6	98.0 ± 1.4	99.2 ± 0.9
	PBS	97.2 ± 1.6	100.3 ± 0.3	99.0 ± 0.3
Refractive index		1.421 ± 0.001	1.423 ± 0.001	1.423 ± 0.001
Water contact angle (°)		55.08 ± 4.60	49.28 ± 1.52	52.56 ± 4.33

($p < 0.0001$). Although the difference is small, lower values of CA values are generally linked to an increase of comfort for the wearer [5, 57,58].

3.3.1. *Thermotropic properties*

Characteristic DSC thermograms obtained for the NT and SCT hydrogels in their dry state are presented in Fig. 5A. The DSC thermograms provide insight into the underlying polymer structure, showing a predominantly endothermic behaviour throughout the tested temperature range. Regarding the monomers used, both HEMA (T_g~83 °C, [59]) and PVP (T_g~175 °C, [60]) have well described T_g values, whereas for TRIS, to date, literature does not explicitly mention any value. The produced hydrogels demonstrate a visible T_g in the range of 175 – 200 °C and a subtle transition around 80 – 100 °C. These may be attributed to PVP and HEMA knowns T_gs, but mainly indicate a possible variation of the thermotropic behaviour of samples due to a degree of structural heterogeneity [61].

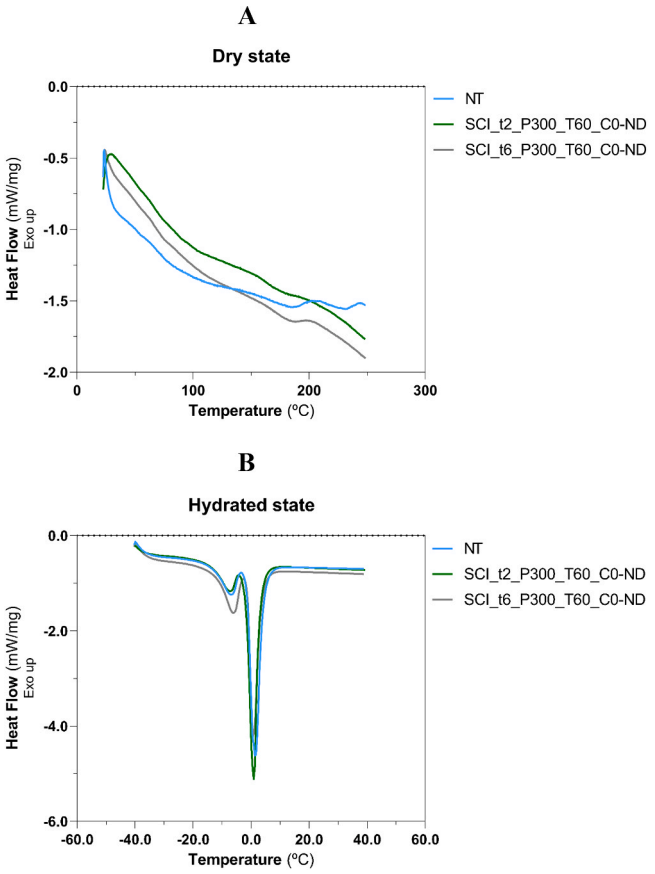

Fig. 5. Representative thermograms obtained by DSC for NT hydrogels, SCI_t2_P300_T60_C0-ND and SCI_t6_P300_T60_C0-ND samples. A) dry state; B) hydrated state.

High crosslinking densities can restrict chain mobility affecting significantly T_g, shifting it to higher temperatures or even surpass the event entirely, making harder to detect in the thermograms [62]. However, the presence of two shifts, suggests the formation of a network with block or phase-separated domains rather than a perfectly homogeneous random sequence [63]. The observation that these transitions remain consistent across both NT and SCT samples confirms that supercritical processing preserves this complex structure.

Fig. 5B shows the results regarding the hydrated samples. As stated by Silva *et al.* [59] three states of water can be found in hydrated hydrogels, i.e., tightly bound water, loosely bound water and free water. The determination of these water states is crucial for assessing the suitability of the hydrogel for the intended application, as the water present will influence the molecular interaction and transport of the drug [60], ultimately defining the therapeutic efficacy of the samples.

All samples demonstrated two endothermic peaks that can be attributed to the fusion of loosely bound water (T < 0 °C) and free water (T ≥ 0 °C) [62]. The estimated fusion enthalpies and are reported in Table 6. SCT resulted in a similar thermotropic behaviour to that of the NT sample. No statistical difference was observed regarding the fusion enthalpies of the loosely and free waters when comparing the NT with the SCT samples as well as the SCT among them (Table S6A and B in Supplementary Information). Considering the fusion enthalpy of water 334 J/g [62], it was determined the amount of free and loosely bound water contained in the samples. The sum of the two corresponds to the freezable water. Taking into account the results of the swelling study it was possible to determine the total amount of water contained in the samples and by subtraction, the amount of non-freezable water (tightly bound). The percentages of both types of water (freezable and non-freezable) are presented in Table 6. In all cases, the amount of non-freezable water is superior to the amount of freezable water, which is not negligible (between 33.6% and 40.1%). Besides, the relative amount of non-freezable water is slightly superior in the SCT samples than in the NT sample.

3.3.2. *Morphology*

The obtained SEM micrographs for NT, SCI_t2_P300_T60_C0-ND and SCI_t6_P300_T60_C0-ND samples are presented in Fig. 6. No differences

Table 6
Fusion enthalpy estimated from the areas of the peaks attributed to loosely bond water and free water in the thermograms obtained for NT, SCI_t2_P300_T60_C0-ND and SCI_t6_P300_T60_C0-ND samples. The error bars are the ± standard deviations (n = 3).

Samples	Fusion enthalpy (J/g)		% freezable water	% non-freezable water
	Loosely bond water	Free water		
NT	28.5 ± 11.1	26.1 ± 0.6	40.1	59.9
SCI_t2_P300_T60_C0-ND	19.92 ± 9.3	25.9 ± 6.1	33.6	66.4
SCI_t6_P300_T60_C0-ND	23.23 ± 5.2	26.7 ± 4.3	37.3	62.7

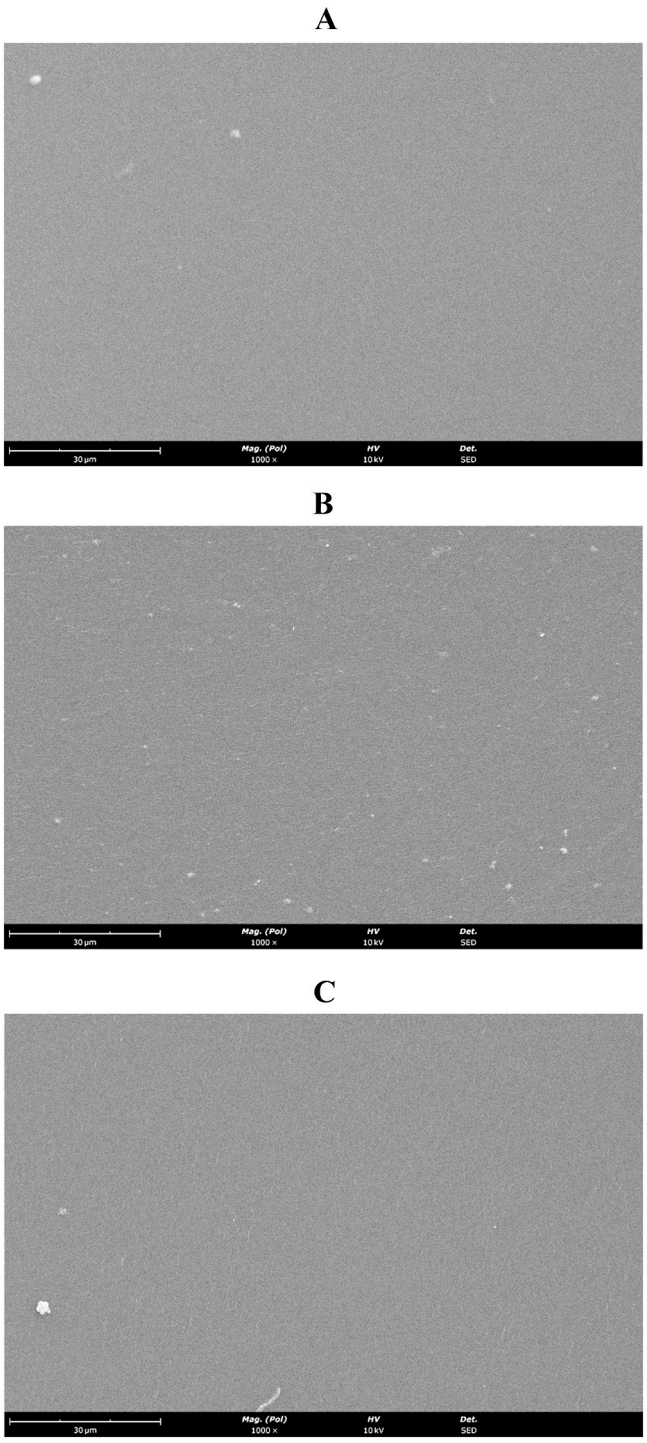

Fig. 6. SEM micrographs of the material's surface A) NT, B) SCI_t2_P300_T60_C0-ND and C) SCI_t6_P300_T60_C0-ND (scale bar: 30 µm) at × 1000 magnification.

between the NT samples and the ones submitted to the SCT could be detected. All samples presented a homogeneous, smooth and flat surface, with no asperities, crevices, or other significant surface morphology features. Comparable features have been observed for hydrogel materials used for contact lenses [50,64]. The produced hydrogels were produced in a mould between two glass plates to ensure a high-quality finish suitable for ophthalmic applications, avoiding possible structural features that could affect optical properties.

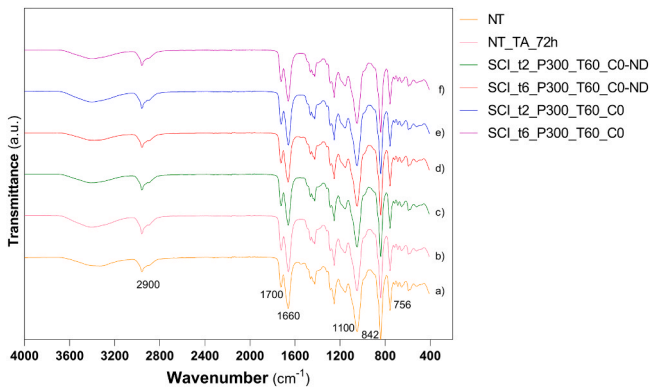

Fig. 7. FTIR-ATR spectra of the not treated hydrogels (NT and NT_TA_72h) and of $scCO_2$ treated without TA (SCI_t2_P300_T60_C0-ND and SCI_t6_P300_T60_C0-ND) and with TA (SCI_t2_P300_T60_C0 and SCI_t6_P300_T60_C0) samples, in the region of 4000–400 cm^{-1}.

3.3.3. Chemical structure

Fig. 7 shows the FTIR spectra of the developed hydrogels both plain (NT, SCI_t2_P300_T60_C0-ND, and SCI_t6_P300_T60_C0-ND) and TA-loaded samples (NT_TA_72h, SCI_t2_P300_T60_C0, SCI_t6_P300_T60_C0). Key peaks were identified and analysed to evaluate the chemical structure of the hydrogel matrix, eventual interactions with the drug and changes due to the SCT.

The results show a broad absorption band around 3400 cm^{-1}, attributed to O–H stretching vibrations that reveals the presence of hydrogen bonding interactions, in both treated (SCI_t2_P300_T60_C0-ND, SCI_t6_P300_T60_C0-ND, SCI_t2_P300_T60_C0 and SCI_t6_P300_T60_C0) and NT hydrogels. This band is characteristic of HEMA due to the presence of hydroxyl groups (-OH) [65,66]. No relevant differences among the different spectra were observed in this region. Distinct peaks around 2900 cm^{-1}, corresponding to aliphatic C-H stretching vibrations, were also observed in all the monomers (see Supplementary Information, Figure S4) and hydrogels confirming the presence of alkyl groups. A strong, sharp peak around 1700 cm^{-1}, corresponding to the stretching vibration of the ester carbonyl group (C═O stretching), was seen in all spectra, being common to the raw materials HEMA and NVP. A prominent absorption band at approximately 1640 cm^{-1} characteristic of the C═C double of the methacrylate group, reveals the presence of the alkene portion of HEMA. In NVP, a peak near 1640 cm^{-1}, also indicative of C═C stretching, is more pronounced due to the contribution of the vinyl groups within its structure [67,68].

In the fingerprint region (1500 – 500 cm^{-1}), multiple sharp peaks between 1300 – 1000 cm^{-1} confirm C-O stretching of ester and ether linkages in HEMA, along with C-N stretching vibrations associated with amine functional group present in TRIS [65]. The C–O–C stretching peak around 1100 cm^{-1}, indicative of ester linkages, confirmed the bonding between the methacrylate and hydroxyethyl groups in HEMA [66]. The antisymmetric stretching of Si–O–Si bond around 1050 cm^{-1} and the Si–$(CH_3)_3$ stretching peaks at 842 cm^{-1} and 756 cm^{-1} highlight the presence of siloxane and trimethylsilyl groups originating from TRIS. Peaks around 800 cm^{-1}, were also identified as being related to the bond Si-O-Si, representing the symmetric stretching of the oxygen bond [69].

Regarding the TA loaded samples, no drug-polymer interactions were observed in the spectra that revealed to be quite similar to the ones obtained for the unloaded samples. The TA spectrum (Supplementary Information, Figure S4) is in accordance with the previously published by Abou-ElNour *et al.* [70]. TA exhibited characteristic absorption bands around 3400 cm^{-1}, corresponding to the stretching of the -OH group. Peaks observed at approximately 2900 cm^{-1} are attributed to C–H stretching. Additional bands appeared at 1700 cm^{-1} and 1660 cm^{-1}, corresponding to C═O stretching of carbonyl groups present in the aliphatic ester and ketone functional groups, as well as C═C stretching.

Furthermore, bands at 1080 cm^{-1} and 1050 cm^{-1} are associated with C–O–C bond stretching and C–F vibrational stretching, respectively. The lack of distinct shifts or new bands suggest a lack of strong chemical interaction between the hydrogels and TA. SCT has been regarded as a promising technique to facilitate and improve the incorporation of therapeutic agents without affecting the chemical structure of the system [71,72]. The fact that no relevant differences were observed in the intensity and position of the peaks between NT samples and the ones submitted to a SCT, also suggests that this process preserved the covalent matrix of the hydrogels, while preventing TA degradation, as could eventually happen [66,73].

Machado *et al.* [74] discussed that for semicyrstalline materials, like the hydrogels in this work, the drug will be incorporated in the amorphous phase. As such, TA molecules are likely molecularly dispersed throughout the matrix, possibly creating intermolecular forces (e.g. Hydrogen bonds). Possible hydrogen bonding between the TA and the polymer units may lead to a broadening of the drug's characteristic peaks, rendering them indistinguishable from the baseline or the hydrogel' own broad bands.

3.3.4. Biocompatibility

3.3.4.1. Irritability test. The results of HET-CAM test are presented in Fig. 8. For both NT and TA-loaded samples (SCI_t2_P300_T60_C0 and SCI_t6_P300_T60_C0), no visual signs of vascular lysis, coagulation, or haemorrhage were observed, similarly to what was seen with the negative control (C^-). In contrast, the positive control (C^+) exhibited clear signs of irritation, which became evident within seconds of the CAM being exposed to the NaOH solution. Hence, the developed SCLs have an IS $= 0.00 \pm 0.00$ (non-irritant), whereas the positive control presents a IS of 20.43 ± 0.32 (severely irritant).

3.3.4.2. Cell viability. Cell viability was determined after indirect contact of the drug-loaded hydrogels with fibroblast cells using the MTT assay (Fig. 9). All samples demonstrated high viability, approaching 100%, thereby confirming that both non-treated and SCI-treated samples were non-cytotoxic.

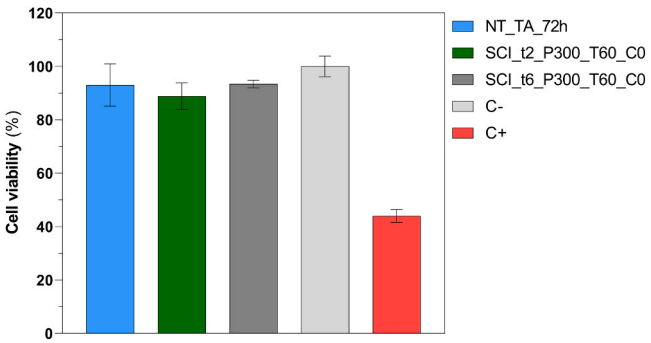

Fig. 9. Cell viability of NIH/3T3 fibroblast cells after indirect contact with NT_TA_72h, SCI_t2_P300_T60_C0 and SCI_t6_P300_T60_C0 hydrogels extracts, evaluated by the MTT assay. Both controls are also shown. Error bars correspond to ± standard deviations (n = 5).

4. Conclusion

Supercritical impregnation of TA in a silicone-base hydrogel for SCLs was successfully carried out. Under the conditions of 60 °C, 300 bar and 6 h, SCI enabled drug loaded amounts of 10.08 ± 1.77 $\mu g.mg^{-1}$ without co-solvent and 11.14 ± 0.57 $\mu g.mg^{-1}$ with 5%v/v co-solvent. Although these values are statistically comparable, a slight increasing trend in loading was observed in the presence of DMSO.

Compared to conventional treatment (6 h soaking), SCI resulted in substantially higher TA loaded amount. While compared to the 72 h conventional impregnation, SCI process lead to a slightly lower drug loading (less 22.5% and 14.4%, respectively). However, drug release studies proved that SCI was more efficient than the conventional impregnation process even after 72 h, yielding increases of 113.3% and 120.0% in released TA, respectively.

A design of experiments through a FFD was used to evaluate the influence of pressure, temperature, impregnation time and amount of co-solvent on the TA cumulative release and loaded amount. Pressure and temperature were found to be the most significant for both responses, whereas co-solvent addition showed limited influence. In general, increasing pressure and temperature enhanced drug release,

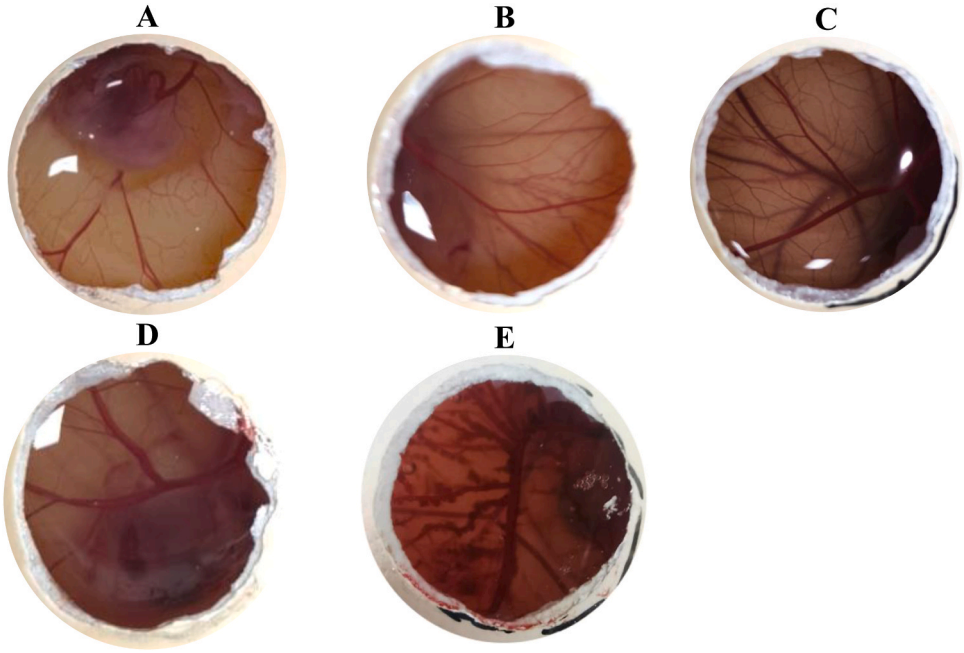

Fig. 8. Images of CAM from hen eggs after 5 min of exposure to: A) NT_TA_72h; B) SCI_t2_P300_T60_C0; C) SCI_t6_P300_T60_C0; D) C^- (0.9% NaCl) and E) C^+ (NaOH 1 M).

with their combined effect demonstrating a synergistic effect being particularly relevant for improving both the impregnation and release of the drug.

The best performing materials were the ones subjected to the harshest conditions of temperature and pressure with a contact time of 6 h (SCI_t6_P300_T60_C5 and SCI_t6_P300_T60_C0) and of 2 h (SCI_t2_P300_T60_C0 and SCI_t2_P300_T60_C5). More, these samples showed suitable optical properties (transmittance above 90% and refractive index of 1.423) and values of swelling ratio, water content and wettability within those found for commercial SCLs. Also, none of the samples induced irritability issues or cytotoxicity.

In conclusion, this work demonstrates the potential of SCI to enhance TA loading in silicon-based hydrogels for SCLs, providing insights to optimise the operating conditions to improve drug release performance. While SCI is a promising alternative to conventional soaking, further research is needed to clarify the underlying transport/partition mechanisms, validate release under physiological tear-flow conditions, and establish scalability and stability for translational use.

Declaration of Competing Interest

The authors declare that they have no known competing financial interests or personal relationships that could have appeared to influence the work reported in this paper.

Acknowledgments

The authors acknowledge Fundação para a Ciência e Tecnologia (FCT) for funding through SOL - Smart ocular lenses for the treatment of diabetic eye diseases (https://doi.org/10.54499/PTDC/CTM-CTM/2353/2021), and through projects of CQE - Centro de Química Estrutural (https://doi.org/10.54499/UID/00100/2025, https://doi.org/10.54499/UID/PRR2/00100/2025 and https://doi.org/10.54499/UID/PRR/00100/2025), of the Associate Laboratory IMS - Institute of Molecular Sciences (https://doi.org/10.54499/LA/P/0056/2020). Diana C. Silva acknowledges FCT for her Junior Research contract 2022.08560.CEECIND/CP1713/CT0016 https://doi.org/10.54499/2022.08560.CEECIND/CP1713/CT0016.

Appendix A. Supporting information

Supplementary data associated with this article can be found in the online version at doi:10.1016/j.supflu.2026.107061.

Data availability

Data will be made available on request.

References

[1] S. Gade, Y. So, D. Mishra, S.M. Baviskar, A.A. Assiri, K. Glover, R. Sheshala, L. K. Vora, R.R.S. Thakur, Ocular drug delivery: emerging approaches and advances, Pharmaceutics 17 (2025) 599, https://doi.org/10.3390/pharmaceutics17050599.
[2] B. Abdi, M. Mofidfar, F. Hassanpour, E.C. Kirbas, S.K. K, P.H. Milani, M. Ghanbarzadeh, D. Fadel, M. Barnett, C.N. T, R.M. Leblanc, A. Chauhan, F. Abbasi, Therapeutic contact lenses for the treatment of corneal and ocular surface diseases: Advances in extended and targeted drug delivery, Int. J. Pharm. 638 (2023) 122740, https://doi.org/10.1016/j.ijpharm.2023.122740.
[3] H. Yang, M. Zhao, D. Xing, J. Zhang, T. Fang, F. Zhang, Z. Nie, Y. Liu, L. Yang, J. Li, D. Wang, Contact lens as an emerging platform for ophthalmic drug delivery: A systematic review, Asian J. Pharm. Sci. 18 (2023) 100847, https://doi.org/10.1016/j.ajps.2023.100847.
[4] M. Drancourt, F. Matonti, Endophthalmitis. Infect. Dis., Elsevier, 2017, pp. 158–164, https://doi.org/10.1016/B978-0-7020-6285-8.00017-4.
[5] I. Rykowska, I. Nowak, R. Nowak, Soft Contact Lenses as Drug Delivery Systems: A Review, Molecules 26 (2021) 5577, https://doi.org/10.3390/molecules26185577.
[6] M. Ioniță, G.M. Vlăsceanu, A.G. Toader, M. Manole, Advances in Therapeutic Contact Lenses for the Management of Different Ocular Conditions, J. Pers. Med. 13 (2023) 1571, https://doi.org/10.3390/jpm13111571.
[7] Y. Tao, J.B. Jonas, Intravitreal triamcinolone, Ophthalmologica 225 (2011) 1–20, https://doi.org/10.1159/000317909.
[8] C. Marto-Costa, N. Toffoletto, M. Salema-Oom, A.M.M. Antunes, C.A. Pinto, A. S. Silva-Herdade, C. Alvarez-Lorenzo, A.P. Serro, Improved triamcinolone acetonide-eluting contact lenses based on cyclodextrins and high hydrostatic pressure assisted complexation, Carbohydr. Polym. 331 (2024) 121880, https://doi.org/10.1016/j.carbpol.2024.121880.
[9] D. Silva, H.C. Sousa, M.H. Gil, L.F. Santos, M. Salema Oom, C. Alvarez-Lorenzo, B. Saramago, A.P. Serro, Moxifloxacin-imprinted silicone-based hydrogels as soft contact lenses materials for extended release, Eur. J. Phar. Sci. 156 (2021) 105591.
[10] A.P. Vieira, A.F.R. Pimenta, D. Silva, M.H. Gil, P. Alves, P. Coimbra, J.L.G. Mata, D. Bozukova, T.R. Correia, I.J. Correia, A.P. Serro, A.J. Guiomar, Surface modification of an intraocular lens material by plasma-assisted grafting with 2-hydroxyethyl methacrylate (HEMA), for controlled release of moxifloxacin, Eur. J. Pharm. Biopharm. 120 (2017) 52–62.
[11] D. Silva, H.C. de Sousa, M.H. Gil, L.F. Santos, G.M. Moutinho, A.P. Serro, B. Saramago, Antibacterial layer-by-layer coatings to control drug release from soft contact lenses material, Int. J. Pharm. 553 (2018) 186–200, https://doi.org/10.1016/j.ijpharm.2018.10.041.
[12] D. Silva, H.C. de Sousa, M.H. Gil, L.F. Santos, R.A. Amaral, J.A. Saraiva, M. Salema Oom, C. Alvarez-Lorenzo, A.P. Serro, B. Saramago, Imprinted hydrogels with LbL coating for dual drug release from soft contact lenses materials, Mat. Sci. Eng. C. 120 (2021) 111687, https://doi.org/10.1016/j.msec.2020.111687.
[13] S.F. Senra, S.R.S. Veloso, M. Lira, E.M.S. Castanheira, Albumin/Hyaluronic Acid Nanoparticle-Laden Contact Lenses for the Ocular Delivery of 5-Fluorouracil, Biomed. Mater. Res. A 113 (2025) e37839, https://doi.org/10.1002/jbm.a.37839.
[14] A. Wong, M. Fallon, V. Celiksoy, S. Ferla, C. Varrichio, D. Whitaker, A.J. Quantock, C.M. Heard, A Composite System Based upon Hydroxypropyl Cyclodextrins and Soft Hydrogel Contact Lenses for the Delivery of Therapeutic Doses of Econazole to the Cornea, In Vitro, Pharmaceutics 14 (2022) 1631, https://doi.org/10.3390/pharmaceutics14081631.
[15] R.R. Horne, K.E. Judd, W.G. Pitt, Rapid loading and prolonged release of latanoprost from a silicone hydrogel contact lens, J. Drug. Deliv. Sci. Technol. 41 (2017) 410–418, https://doi.org/10.1016/j.jddst.2017.08.011.
[16] O.L. Lanier, K.G. Christopher, R.M. Macoon, Y. Yu, P. Sekar, A. Chauhan, Commercialization challenges for drug eluting contact lenses, Expert. Opin. Drug. Deliv. 17 (2020) 1133–1149, https://doi.org/10.1080/17425247.2020.1787983.
[17] X. Fan, C. Torres-Luna, M. Azadi, R. Domszy, N. Hu, A. Yang, A.E. David, Evaluation of commercial soft contact lenses for ocular drug delivery: A review, Acta Biomater. 115 (2020) 60–74, https://doi.org/10.1016/j.actbio.2020.08.025.
[18] P. Chakravarty, A. Famili, K. Nagapudi, M.A. Al-Sayah, Using supercritical fluid technology as a green alternative during the preparation of drug delivery systems, Pharmaceutics 11 (2019) 629, https://doi.org/10.3390/pharmaceutics11120629.
[19] J. Xu, Y. Xue, G. Hu, T. Lin, J. Gou, T. Yin, H. He, Y. Zhang, X. Tang, A comprehensive review on contact lens for ophthalmic drug delivery, J. Control. Release 281 (2018) 97–118, https://doi.org/10.1016/j.jconrel.2018.05.020.
[20] V.P. Costa, M.E.M. Braga, C.M.M. Duarte, C. Alvarez-Lorenzo, A. Concheiro, M. H. Gil, H.C. de Sousa, Anti-glaucoma drug-loaded contact lenses prepared using supercritical solvent impregnation, J. Supercrit. Fluids 53 (2010) 165–173, https://doi.org/10.1016/j.supflu.2010.02.007.
[21] M.E.M. Braga, V.P. Costa, M.J.T. Pereira, P.T. Fiadeiro, A.P. a R. Gomes, C.M. M. Duarte, H.C. De Sousa, Effects of operational conditions on the supercritical solvent impregnation of acetazolamide in Balafilcon A commercial contact lenses, Int. J. Pharm. 420 (2011) 231–243, https://doi.org/10.1016/j.ijpharm.2011.08.040.
[22] V.C. Costa, M.E.M. Braga, J.P. Guerra, A.R.C. Duarte, C.M.M. Duarte, E.O.B. Leite, M.H. Gil, H.C. de Sousa, Development of therapeutic contact lenses using a supercritical solvent impregnation method, J. Supercrit. Fluids 52 (2010) 306–316, https://doi.org/10.1016/j.supflu.2010.02.001.
[23] F. Yañez, L. Martikainen, M.E. Braga, Supercritical fluid-assisted preparation of imprinted contact lenses for drug delivery, Acta Biomater. 7 (2011) 1019–1030, https://doi.org/10.1016/j.actbio.2010.10.003.
[24] Y. Yokozaki, Y. Shimoyama, Loading of vitamin E into silicone hydrogel by supercritical carbon dioxide impregnation toward controlled release of timolol maleate, J. Supercrit. Fluids 131 (2018) 11–18, https://doi.org/10.1016/j.supflu.2017.08.010.
[25] H. Erdogan, B. Gungor, S.S. Suner, C. Silan, S.U. Saraydin, D. Saraydin, R.S. Ayyala, S. Nurettin, Moxifloxacin-Impregnated Contact Lenses for Treatment of Keratitis in Rabbit Eyes, Polym. Adv. Technol. 36 (2025) e70134, https://doi.org/10.1002/pat.70134.
[26] H.C. de Sousa, M.M. Gil, C.M. Duarte, E.B. Leite, A.C. Duarte, Method for preparing therapeutic ophthalmic articles using compressed fluids, EP1611877A1 (2006).
[27] C. González-Chomón, M.E.M. Braga, H.C. de Sousa, A. Concheiro, C. Alvarez-Lorenzo, Antifouling foldable acrylic IOLs loaded with norfloxacin by aqueous soaking and by supercritical carbon dioxide technology, Eur. J. Pharm. Biopharm. 82 (2012) 383–391, https://doi.org/10.1016/j.ejpb.2012.07.007.
[28] K. Ongkasin, Y. Masmoudi, T. Tassaing, G. Le-Bourdon, E. Badens, Supercritical loading of gatifloxacin into hydrophobic foldable intraocular lenses – Process control and optimization by following in situ CO2 sorption and polymer swelling, Int. J. Pharm. 581 (2020) 119247, https://doi.org/10.1016/j.ijpharm.2020.119247.
[29] M.A.T. Cardoso, G.A. Monteiro, J.P. Cardoso, T.J.V. Prazeres, J.M.F. Figueiredo, J. M.G. Martinho, J.M.S. Cabral, A.M.F. Palavra, Supercritical antisolvent micronization of minocycline hydrochloride, J. Supercrit. Fluids 44 (2008) 238–244, https://doi.org/10.1016/j.supflu.2007.09.035.
[30] G. Sodeifan, R.S. Alwi, M.A. Nooshabadi, F. Razmimanesh, A. Roshanghias, Solubility measurement of Triamcinolone acetonide (steroid medication) in

supercritical CO2: Experimental and thermodynamic modeling, J. Supercrit. Fluids 204 (2024) 106119, https://doi.org/10.1016/j.supflu.2023.106119.
[31] A. Topete, B. Saramago, A.P. Serro, Intraocular lenses as drug delivery devices, Int. J. Pharm. 602 (2021) 120613, https://doi.org/10.1016/j.ijpharm.2021.120613.
[32] N.F. Ramandi, N.M. Najafi, F. Raofie, E. Ghasemi, Central composite design for the optimization of supercritical carbon dioxide fluid extraction of fatty acids from Borago officinalis L. flower, C1262-6, J. Food Sci. 76 (2011), https://doi.org/10.1111/j.1750-3841.2011.02394.x.
[33] M. Champeau, J.-M. Thomassin, T. Tassaing, C. Jérôme, Drug loading of polymer implants by supercritical CO2 assisted impregnation: A review, J. Control. Release 209 (2015) 248–259, https://doi.org/10.1016/j.jconrel.2015.05.002.
[34] ICCVAM-Recommended Test Method Protocol: Hen's Egg Test – Chorioallantoic Membrane (HET-CAM) Test Method, (2010). https://doi.org/http://iccvam.niehs.nih.gov/methods/ocutox/MildMod-TMER.htm.
[35] L.V. Garcia, D. Silva, M.M. Costa, H. Armés, M. Salema-Oom, B. Saramago, A. P. Serro, Antiseptic-Loaded Casein Hydrogels for Wound Dressings, Pharmaceutics 15 (2023) 1–24, https://doi.org/10.3390/pharmaceutics15020334.
[36] ISO 10993-5:2009 - Biological evaluation of medical devices — Part 5: Tests for in vitro cytotoxicity, ISO (International Organ. Stand. (n.d.). ⟨https://www.iso.org/obp/ui#iso:std:iso:10993:-5:ed-3:v1:en⟩ (accessed June 30, 2025).
[37] M. Dippold, H. Ruckdäschel, Influence of pressure-induced temperature drop on the foaming behavior of amorphous polylactide (PLA) during autoclave foaming with supercritical CO2, J. Supercrit. Fluids 190 (2022) 105734, https://doi.org/10.1016/j.supflu.2022.105734.
[38] M. Champeau, J. Thomassin, C. Jérôme, T. Tassaing, situs investigation of supercritical CO2 assited impregnation of drugs into a polymer by high pressure FTIR microspectroscopy, Analyst 140 (2015) 869, https://doi.org/10.1039/C4AN01130A.
[39] O.I. Gromov, M.O. Kostenko, A.V. Petrunin, A.A. Popova, O.O. Parenago, N. V. Minaev, E.N. Golubeva, M.Y. Melnikov, Solute Diffusion into Polymer Swollen by Supercritical CO2 by High-Pressure Electron Paramagnetic Resonance Spectroscopy and Chromatography, Polymers 13 (2021) 3059, https://doi.org/10.3390/polym13183059.
[40] M. Perrut, V. Perrut, Towards ingredients by combining Supercritical Fluids with other processes, J. Supercrit. Fluids 134 (2018) 214, https://doi.org/10.1016/j.supflu.2017.11.019.
[41] S. Cardea, E. Reverchon, Supercritical fluid processing of polymers, Plymers 11 (2019) 1551, https://doi.org/10.3390/polym11101551.
[42] W. Stiver, Chrastil revisited for supercritical carbon dioxide, J. Supercrit. Fluids 177 (2021) 105348, https://doi.org/10.1016/j.supflu.2021.105348.
[43] M.V. Natu, M.H. Gil, H.C. de Sousa, Supercritical solvent impregnation of poly (ε-caprolactone)/poly (oxyethylene-b-oxypropylene-b-oxyethylene) and poly (ε-caprolactone)/poly (ethylene-vinyl acetate) blends for controlled release applications, J. Supercrit. Fluids 47 (2008) 93–102, https://doi.org/10.1016/j.supflu.2008.05.006.
[44] H.R. Azimi, M. Rezaei, Solubility and diffusivity of carbon dioxide in St-MMA copolymers, J. Chem. Thermodyn. 58 (2013) 279–287, https://doi.org/10.1016/j.jct.2012.11.025.
[45] D. Elustondo, L. Raymond, R. Risani, L. Donaldson, M.J. Le Guen, Exploratory Pressure Impregnation Process Using Supercritical CO2, Co-Solvents, and Multi-Cycle Implementation, Forests 13 (2022) 2018, https://doi.org/10.3390/f13122018.
[46] K. Ongkasin, Y. Masmoudi, C.M. Wertheimer, A. Hillenmayer, K.H. Eibl-Lindner, E. Badens, Supercritical fluid technology for the development of innovative ophthalmic medical devices: Drug loaded intraocular lenses to mitigate posterior capsule opacification, Eur. J. Pharm. Biopharm. 149 (2020) 248–256, https://doi.org/10.1016/j.ejpb.2020.02.011.
[47] A. Bouledjouidja, Y. Masmoudi, M. Sergent, E. Badens, Effect of operational conditions on the supercritical carbon dioxide impregnation of anti-inflammatory and antibiotic drugs in rigid commercial intraocular lenses, J. Supercrit. Fluids 130 (2017) 63–75, https://doi.org/10.1016/j.supflu.2017.07.015.
[48] P.A. Uwineza, A. Waśkiewicz, Recent Advances in Supercritical Fluid Extraction of Natural Bioactive Compounds from Natural Plant Materials, Molecules 25 (2020) 3847, https://doi.org/10.3390/molecules25173847.
[49] A.F.R. Pimenta, A.P. Serro, R. Colaço, A. Chauhan, Optimization of intraocular lens hydrogels for dual drug release: Experimentation and modelling, Eur. J. Pharm. Biopharm. 141 (2019) 51–57, https://doi.org/10.1016/j.ejpb.2019.05.016.
[50] N.-P.-D. Tran, M.-C. Yang, Synthesis and characterization of silicone contact lenses based on TRIS-DMA-NVP-HEMA hydrogels, Polymers 11 (2019) 944, https://doi.org/10.3390/polym11060944.
[51] S. Cascone, G. Lamberti, Hydrogel-based commercial products for biomedical applications: a review, Int. J. Pharm. 573 (2020) 118803, https://doi.org/10.1016/j.ijpharm.2019.118803.
[52] S. Chatterjee, P. Upadhyay, M. Mishra, M. Srividya, M.R. Akshara, N. Kamali, Z. S. Zaidi, S.F. Iqbal, S.K. Misra, Advances in chemistry and composition of soft materials for drug releasing contact lenses, RSC Adv. 10 (2020) 36751, https://doi.org/10.1039/d0ra06681h.
[53] C.C.S. Karlgard, N.S. Wong, L.W. Jones, C. Moresoli, vitro uptake and release studies of ocular pharmaceutical agents by silicon-containing and p-HEMA hydrogel contact lens materials, Int. J. Pharm. 257 (2003) 141–151, https://doi.org/10.1016/s0378-5173(03)00124-8.
[54] S. Patel, L. Tuchenko, The refractive index of the human cornea: A review, Cont. Lens Anterior Eye 42 (2019) 575–580, https://doi.org/10.1016/j.clae.2019.04.018.
[55] José M. González-Méijome, Antonio López-Alemany, Madalena Lira, José B. Almeida, Elisabete C.D. Real Oliveira, Manuel A. Parafita, Equivalences between refractive index and equilibrium water content of conventional and silicone hydrogel soft contact lenses from automated and manual refractometry abstract refractometry, J. Biomed. Mater. Res. Part. B Appl. Biomater. (2006) 184–191, https://doi.org/10.1002/jbm.b.30583.
[56] D. Silva, H.C. de Sousa, M.H. Gil, L.F. Santos, G.M. Moutinho, M. Salema-Oom, C. Alvarez-Lorenzo, A.P. Serro, B. Saramago, Diclofenac sustained release from sterilised soft contact lens materials using an optimised layer-by-layer coating, Int. J. Phar 585 (2020) 119506, https://doi.org/10.1016/j.ijpharm.2020.119506.
[57] A. Guzman-Aranguez, B. Colligris, J. Pintor, Contact lenses: promising devices for ocular drug delivery, J. Ocul. Pharmacol. Ther. 29 (2013) 189–199, https://doi.org/10.1089/jop.2012.0212.
[58] H. Gohel P, G. Shahbaz, V. Shah, U.M. Upadhyay, Drug-eluting therapeutic contact lens, Int. J. Pharm. Res. Allied Sci. 1 (2012) 1–6.
[59] A. Marcinkowaska, D. Przadka, E. Andrzejewska, Modification of poly-HEMA with nonreactive POSS derivatives by in situ photopolymerization, J. Therm. Anal. Calorim. 138 (2018) 1033–1047, https://doi.org/10.1007/s10973-019-08178-9.
[60] A. Angelini, C. Fodor, L. Leva, A. Car, I.A. Dinu, W. Yave, W. Meier, Synthesis and characterization of tailor-made N-vinylpyrrolidone copolymers and their blend membranes with polyvinyl alcohol for bioethanol dehydration by pervaporation, J. Appl. Polym. Sci. 139 (2022) e51562, https://doi.org/10.1002/app.51562.
[61] T. Caykara, Ö. Kantoglu, T. Çaykara, C. Özyürek, Ö. Kantoglu, Investigation of thermal behavior of poly(2-hydroxyethylmethacrylate-co-itaconic acid) Networks, J. Appl. Polym. Sci. 103 (2007) 681–689, https://doi.org/10.1002/app.24522.
[62] R. Huang, K. Zhao, P. Cao, L. Cao, H. Liao, X. Tang, Molecular Simulation Study on the Impact of a Cross-Linked Network Structure on the Tensile Mechanical Properties of PBT Substrates, Materials 18 (2025) 1675, https://doi.org/10.3390/ma18071675.
[63] L.W. Taylor, R.D. Priestley, R.A. Register, Impact of Monomer Sequence and Interaction Parameter on Polymer Glass Transition Temperature, J. Phys. Chem. B. 129 (2025) 9485–9494, https://doi.org/10.1021/acs.jpcb.5c03909.
[64] D. Silva, A.C. Fernandes, T.G. Nunes, R. Colaço, A.P. Serro, The effect of albumin and cholesterol on the biotribological behaviour of hydrogels for contact lenses, Acta Biomater. 26 (2015) 184–194, https://doi.org/10.1016/j.actbio.2015.08.011.
[65] L. Nebhani, A. Jaisingh, Chemical analysis of polymers. Polym. Sci. Innov. Appl, Elsevier, 2020, pp. 69–116, https://doi.org/10.1016/B978-0-12-816808-0.00003-2.
[66] M. Fathi, G. Sodeifian, S.A. Sajadian, Experimental study of ketoconazole impregnation into polyvinyl pyrrolidone and hydroxyl propyl methyl cellulose using supercritical carbon dioxide: Process optimization, J. Supercrit. Fluids 188 (2022) 105674, https://doi.org/10.1016/j.supflu.2022.105674.
[67] B.A. Trofimov, N.I. Golovanova, A.I. Mikhaleva, S.E. Korostova, A.N. Vasil'ev, L. N. Balabanova, IR spectra of substituted pyrroles, Chem. Heterocycl. Compd. 13 (1977) 734–738, https://doi.org/10.1007/BF00470191.
[68] X. Yu, Y. Xiong, Z. Li, H. Tang, Preparation and Characterization of Tris (trimethylsiloxy)silyl Modified Polyurethane Acrylates and Their Application in Textile Treatment, Polym. (Basel) 12 (2020) 1629, https://doi.org/10.3390/polym12081629.
[69] N.J. Curtis, J.R. Gascooke, A. Pring, Silicon-oxygen region infrared and raman analysis of opals: the effect of sample preparation and measurement type, Minerals 11 (2021) 173, https://doi.org/10.3390/min11020173.
[70] M. Abou-ElNour, R.A.H. Ishak, M. Tiboni, G. Bonacucina, M. Cespi, L. Casettari, M. E. Soliman, A.S. Geneidi, Triamcinolone acetonide-loaded PLA/PEG-PDL microparticles for effective intra-articular delivery: synthesis, optimization, in vitro and in vivo evaluation, J. Control. Release 309 (2019) 125–144, https://doi.org/10.1016/j.jconrel.2019.07.030.
[71] A.B.S. Rosa, S. Marceneiro, M.E.M. Braga, A.M.A. Dias, Solubility of all-trans retinoic acid in supercritical carbon dioxide, J. Supercrit. Fluids 98 (2015) 70–78, https://doi.org/10.1016/j.supflu.2014.12.027.
[72] K.A. Kravanja, M. Finšgar, Ž. Knez, M.K. Marevci, Supercritical Fluid Technologies for the Incorporation of Synthetic and Natural Active Compounds into Materials for Drug Formulation and Delivery, Pharmaceutics 14 (2022) 1670, https://doi.org/10.3390/pharmaceutics14081670.
[73] S.G. Kazarian, G.G. Martirosyan, Spectroscopy of polymer/drug formulations processed with supercritical fluids: in situ ATR–IR and Raman study of impregnation of ibuprofen into PVP, Int. J. Pharm. 232 (2002) 81–90, https://doi.org/10.1016/S0378-5173(01)00905-X.
[74] N.D. Machado, J.E. Mosquera, R.E. Martini, M.L. Goñi, N.A. Gañan, Supercritical CO2-assisted impregnation/deposition of polymeric materials with pharmaceutical, nutraceutical, and biomedical applications: A review (2015–2021), J. Supercrit. Fluids 191 (2022) 105763, https://doi.org/10.1016/j.supflu.2022.105763.